MichiganTech
Create the Future

Michigan Technological University

Digital Commons @ Michigan Tech

Dissertations, Master's Theses and Master's Reports - Open

Dissertations, Master's Theses and Master's Reports

2008

Electronic properties of zig-zag carbon nanotubes : a first-principles study

Pavan Kumar Valavala
Michigan Technological University

Follow this and additional works at: https://digitalcommons.mtu.edu/etds

Part of the Physics Commons

Recommended Citation

Valavala, Pavan Kumar, "Electronic properties of zig-zag carbon nanotubes : a first-principles study", Master's Thesis, Michigan Technological University, 2008.
https://digitalcommons.mtu.edu/etds/119

Follow this and additional works at: https://digitalcommons.mtu.edu/etds

Part of the Physics Commons

ELECTRONIC PROPERTIES OF ZIG-ZAG CARBON NANOTUBES: A *FIRST-*

PRINCIPLES STUDY

By

PAVAN KUMAR VALAVALA

A THESIS

Submitted in partial fulfillment of the requirements

for the degree of

MASTER OF SCIENCE

(Physics)

MICHIGAN TECHNOLOGICAL UNIVERSITY

2008

This thesis, "Electronic Properties of Zig-Zag Carbon Nanotubes: A *First-Principles Study*," is hereby approved in partial fulfillment of the requirements for the degree of MASTER OF SCIENCE in the field of Physics.

DEPARTMENT:

Physics

Signatures:

Thesis Advisor _____

Typewritten Name: Prof. Ranjit Pati

Thesis Co-Advisor_____

Typewritten Name: Prof. Gregory M. Odegard

_____

Department Chair   Prof. Ravindra Pandey

Date   _____

Acknowledgements

I would like to express a few heart felt words to the people who have been a part of this research in numerous ways, people who showed unrelenting support during my work at Michigan Technological University.

My sincere thanks to Prof. Ranjit Pati, for advising me on academic and personal issues throughout the program; to Prof. Gregory Odegard, and Prof. Max Seel for their valuable guidance and for being on my thesis committee. I am grateful to all my colleagues at Prof. Pati's Laboratory and Computational Mechanics and Materials Research Laboratory (CMMRL) for their support and assistance at various stages of this research. Most importantly, I will always be indebted to my family for their support and encouragement to pursue my dreams. Finally, I would like to express my appreciation for all the readers of this manuscript, who I hope will find it useful and carry on the work with same dedication and integrity I have valued in all the above mentioned people.

Abstract

Carbon nanotube (CNT) is a one dimensional (1-D) nanostructured material, which has been the focal point of research over the past decade for intriguing applications ranging from nanoelectronics to chemical and biological sensors. Using a first-principles gradient corrected density functional approach, we present a comprehensive study of the geometry and energy band gap in zig-zag semi-conducting (n,0) carbon nanotubes (CNT) to resolve some of the conflicting findings. Our calculations confirm that the single wall (n,0) CNTs fall into two distinct classes depending upon n mod 3 equal to 1 (smaller band gaps) or 2 (larger gaps). The effect of longitudinal strain on the band gap further confirms the existence of two distinct classes: for n mod 3 = 1 or 2, changing E_g by ~ ±110 meV for 1% strain in each case. We also present our findings for the origin of metallicity in multiwall CNTs.

Table of Contents

Chapter 1

Introduction

Since the beginning of civilization, materials have defined substantially periods of history that brought about insurmountable changes through the use of certain materials. Archeologists broadly classify prehistory into three eras: the Stone Age, the Bronze Age, and the Iron Age [1]. Each period is known for advancements enabled by the efficient use of materials as tools that shaped the contemporary world. The Stone Age is characterized by the use of tools crafted from stone that assisted primitive civilizations to hunt and gather food. The Bronze Age was dominated by the use of copper and bronze and was led to the inception of metalworking. The Iron Age is marked by the widespread use of cast iron tools for various activities. It is undisputable that materials play a vital role in the advancement of the quality of human life. The evolution of global connectivity has heavily relied on the use of solid-state devices in various electronics.

One of the primary focuses of contemporary research is to understand matter from a fundamental standpoint that can potentially lead to designing many novel devices and structures. Nanoscience refers to the study of matter at the atomic or molecular scale

(typically 100 nm or smaller). Nanoscience has opened doors to many fields of inter-disciplinary research spanning the entire spectrum from basic sciences to engineering. In 1959, Nobel laureate Richard P. Feynman delivered a talk at the American Physical Society at Caltech titled "There's plenty of room at the bottom"[2]. This lecture was a solicitation to the innumerable opportunities in the uncharted area of nanoscience.

1.1   CARBON NANOMATERIALS

Nanomaterial is a term used broadly for materials that have been synthesized to possess a certain characteristics by design at the namometer scale to achieve certain desired properties. In 1985, a group of five scientists from Rice University discovered a new carbon allotrope known as "C_{60}: Buckminsterfullerene"[3]. This work was awarded the Nobel prize in Chemistry in 1996 [4]. Following the discovery of "fullerenes", in 1991 a Japanese scientist discovered carbon nanotube (also considered an allotrope of carbon) [5]. A Carbon nanotube (CNT) is a one dimensional (1-D) nanostructured material, which has been the focal point of research over the past decade for intriguing applications ranging from nanoelectronics to chemical and biological sensors. The geometry of the carbon nanotube is uniquely described by a chiral vector $(\vec{C}): \vec{C} = n\vec{a} + m\vec{b}$, denoted by a pair of indices (n, m) that connect the two crystallographically equivalent sites on the graphene sheet (a single layer of graphite). CNTs can be classified based on the chiral indices (n,m) that define its geometry. When

either *n* or *m* is equal to zero, rolling a graphene sheet results in a "zig-zag" CNT. In cases, when *n* = *m*, the resultant CNT is known have an "armchair" configuration, all the other cases when (*n* ≠ *m*) is referred to as "chiral" structure. Figure 1.1 is a graphic representation of the various kinds of CNT based on its geometry. In addition to C_{60} and CNT, other forms of carbon include diamond, graphite, and amorphous carbon.
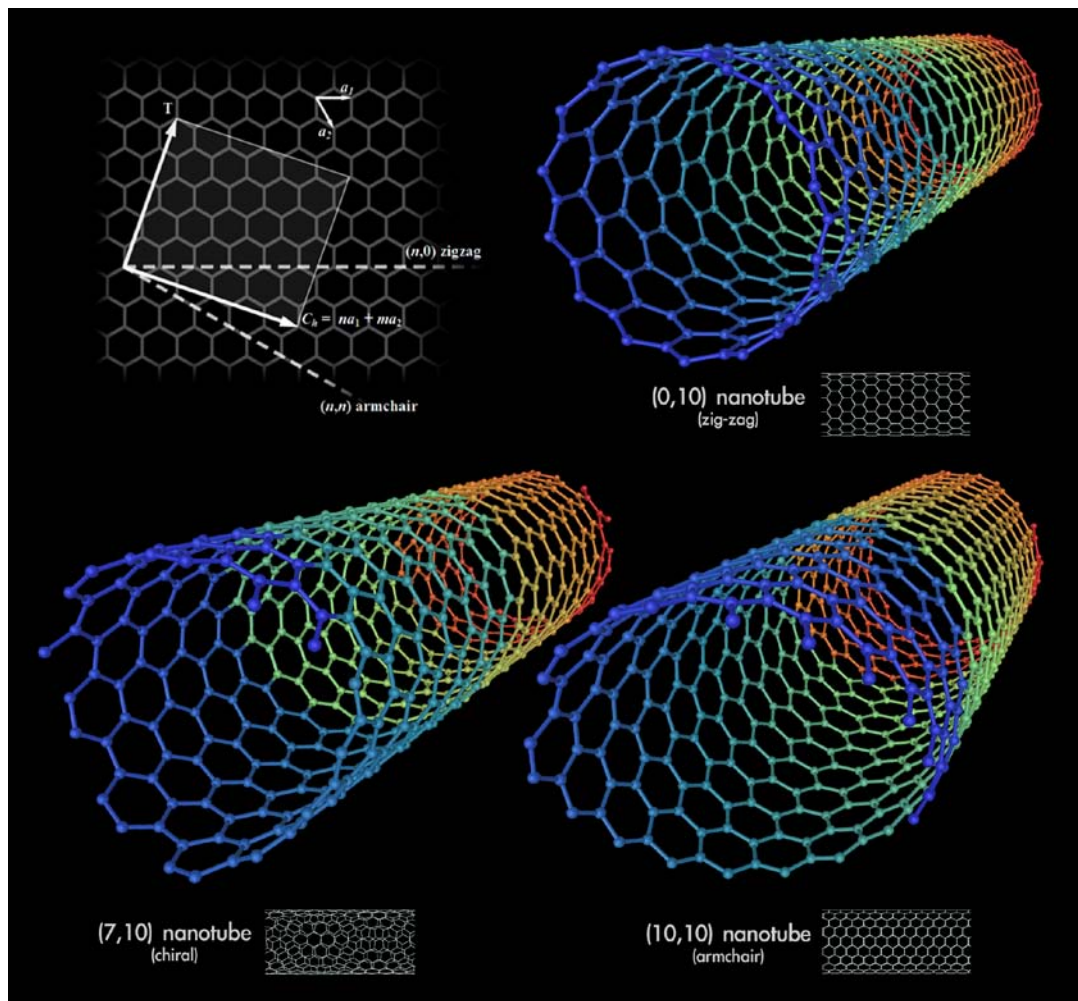

Figure 1.1 A graphic representation of different kinds of CNT based on its chiral indices *(n,m)* (accessed on July 10, 2008; Copyright - Michael Ströck, Wikimedia Commons, 2006, distributed under GFDL, refer Appendix A for permission) [6]

1.2   APPLICATIONS OF CARBON NANOTUBES

It was reported that depending on the chirality of the CNT its electronic properties change. It was also found that it possessed exceptional mechanical, electrical and optical properties that made it an excellent candidate for numerous applications that spawned a great interest in this form of carbon.

A. *Structural Applications*

Due to their chemical structure honeycomb arrangement of the carbon atoms and a extremely high degree of symmetry CNTs possess excellent mechanical properties. It is found that the strength and stiffness of this material far exceeds that of steel and ability to withstand much larger strains to failure resulting is extremely tough behavior [7-9]. Also, carbon nanotubes are much lighter than steel making them ideal for reinforcements in polymer matrix composites [10-15]. Some interesting application for CNT have suggested in view of its exceptional mechanical properties such as the space elevator.

B. *Electronics Applications*

CNTs posses' unique characteristics in terms of their electronic properties, the chilarity of a CNT determines its eventual properties. This unique dependence makes it conducive to certain applications in nanoscale electronics or molecular electronics. In addition, it has also been shown that CNT can be used a capacitor that has potential for

11

commercial batteries [16]. Researchers have also found excellent field emission (emission of electrons from surface in presence of high electric fields) properties for CNT making it ideal for microelectronic devices and certain advanced microscopy techniques [17]. It is also tolerant to faults without significant impact on its performance when compared to silicon.

C. Chemical and Biological Applications

Single walled CNTs show significant changes in their electrical properties when exposed to certain chemical environments making them suitable for chemical sensing. It was also reported that these devices exhibit much higher sensitivity than the current solid-state sensors used for the application [18].

An understanding of binding of certain molecules to specific proteins can pave the road for deigning novel medicine or molecular medicine. An extremely high aspect ratio of the CNT provides a large surface area for effective detection of certain biomolecules even at a very low concentration making it ideal for applications such as drug delivery [19]. The applications of CNT in biology are not restricted to sensing, self powered artificial muscles and prosthetics are envisioned to be potential applications [20]. It has been reported that CNT based artificial muscles for robotics applications can be manufactured from sheets of CNT that can store energy while not in use due its function as a capacitor [21].

1.3   OBJECTIVE

One of the central requirements for a device to operate according to predetermined design relies on *apriori* accurate knowledge of the characteristics of the components. Numerous applications for CNTs rely on its novel electrical properties and experimental determination of their chiralities and measurement of their diameters has been a challenge. These characteristics are crucial to its overall performance as they can vary significantly. A third of the single walled CNTs are metallic while the rest are semiconducting. It is extremely difficult to control the chiralities of the CNTs as grown in laboratory. A vital part of the manufacture process is characterization of the synthesized tubes. The experimental measurements fall within the accuracy of the measuring techniques making it extremely difficult to make a unique characterization. However, *apriori* information of their properties can aide in design of reliable and efficient characterization as well as purification processes. Computational solid-state physics provides the tools to probe the properties of these materials with minimal experimental data. Computational studies in conjunction with experiments can help exploit the potential of CNTs. **The objective of the current research is to explore certain aspects of the electronic properties of CNTs via *first-principles* simulations. First, the exact dependence of chirality of a zig-zag semiconducting CNT on its energy band gap will be explored. And second, the role of the electronic properties of individual wall of a multiwall CNT on its overall behavior will be presented.**

Chapter 2

First-Principles Simulation

Techniques

Condensed matter physics is a field of physical science that is used to describe the study of matter in its "condensed" state generally associated with solids and liquid phase materials. One of the categories in this area that strives to understand matter in solid phase is known as solid-state physics. This discipline of science relies on a large number of experimental, theoretical and computational techniques to probe the properties to better understand materials. An area that involves extensive use of computational techniques is exploring electronic properties of solid state matter. Electronic properties can be studied at various length scales spanning from macro-scale to sub-atomic scales with distinct characteristics at every length scale. Many physical and chemical properties manifested at the macroscale can be related back to the arrangement of electrons at the atomic scale.

In the beginning of the 20th century, physicists were struggling to explain certain experimentally observed phenomenon as black body radiation and spectrum of certain

atoms using classical or Newtonian mechanics. Classical mechanics is extremely successful in describing the working of the macroscale however; these rules were violated at the smaller length scale and anomalies were observed. This behavior of matter at atomic and sub-atomic scales demanded the formulation of a theory that is capable of describing experimentally results. Over the next few decades a number of physicists have been able to comprehend experimental observations based on "quantum mechanics". Quantum mechanics is a probabilistic description of mechanical systems at the atomic and subatomic scales.

2.1   SCHRÖDINGER EQUATION

One of the corner stone's of quantum mechanics is the Schrödinger equation, which a fundamental description of time evolution of quantum state of a system. This opened doors to a more comprehensive understanding of physical and chemical properties of matter. Equation (2.1) represents a time independent Schrödinger equation. In the context of electrons, Schrödinger equation represents a wavefunction. Equation (2.2) is the Hamiltonian for a many body problem neglecting the relativistic effects. Despite its ability to explain many interesting phenomenon, the Schrödinger equation cannot be solved in closed form beyond one-electron systems severely restricting its application. Most solids are rather large systems with multiple molecules that are made of atoms that in turn consist of numerous electrons. The solution of Schrödinger equation for such systems holds the key to its properties, this many body problem does not have an

analytic solution. To circumvent this problem, one has to rely on approximate solutions to the Schrödinger equation.

$$\hat{H}\left|\Psi\right\rangle = E\left|\Psi\right\rangle \qquad (2.1)$$

where, $\hat{H}$ is the Hamiltonian operator, E is the energy eigenvalue of the system and $\left|\Psi\right\rangle$ is the electron wave function. For a general case where Ψ represents a N-electron wavefunction $\left|\Psi\right\rangle = \Psi\left(\vec{r}_1, \vec{r}_2, \ldots, \vec{r}_N\right)$.

$$\hat{H} = -\sum_i \frac{1}{2}\nabla_i^2 - \sum_K \frac{1}{2M_K}\nabla_K^2 - \sum_{i,K} \frac{Z_K}{\left|\vec{r}_i - \vec{R}_K\right|} + \sum_{i>j} \frac{1}{\left|\vec{r}_i - \vec{r}_j\right|} + \sum_{K>L} \frac{Z_K Z_L}{\left|\vec{R}_K - \vec{R}_L\right|} \qquad (2.2)$$

where, the terms involving ∇^2 represent the kinetic energies of the electrons and nuclei for the subscript i and K respectively. Z represents the number of protons in the nuclei; r and R are the position vectors for the nuclei and the electron respectively. M is the mass of the nucleus.

2.2 BORN-OPPENHEIMER APPROXIMATION

The Schrödinger equation in its time-independent non-relativistic form involves the kinetic energy of the nuclei of the physical system. It is well known that the mass of an atom is primarily concentrated in its nucleus and the electrons constitute a very minor percentage of the overall mass of the atom. In most cases, the speeds which the electrons orbit the nucleus is much higher than the speed at which the nucleus is moving. In light of these observations, it can argued that the kinetic energy of the nuclei

have a very negligible contribution to the overall energy of the system and hence can be ignored. In the absence of nuclear kinetic energy, equation (2.2) can be written as.

$$\hat{H} = \hat{T}_e + \hat{J} \qquad (2.3)$$

where, $\hat{T}_e$ is the kinetic energy of the electrons in the system and $\hat{J}$ represents the Coulombic interactions including electron-electron, nucleus-nucleus and nucleus-electron interactions.

In essence, Born-Oppenheimer approximation freezes the nuclei in space and thereby creating a constant potential. Equation (2.3) reduces the complexity of the many body problem, however, it still does not lend itself to be solved in closed form, many approximations have been proposed and are required for a solution to this highly coupled problem. Some of the widely accepted methods are discussed in the following sections.

2.3   HARTREE-FOCK METHOD

The solution of the Schrödinger equation to these complex physical systems can be obtained from various methods. Each of these methods provide certain strengths and weakness making them suitable for specific applications and the level of complexity involved in applying these methods also varies. Soon after the Schrödinger proposed the wave equation in 1926, Douglas Hartree introduced a numerical procedure to solve the

Schrödinger's equation; he proposed that the many body wavefunction can be written as a product of the hydrogen like wavefunctions. It is analogous to the linear combination of atomic orbitals (LCAO) methodology employed in some calculated today. This came to be known as the Hartree product and the procedure was termed the self-consistent field method. However, it did not take the principle of anti-symmetry (put forth by Wolfgang Pauli for fermions) of the electron wavefunction into account. It was later shown that if the one particles wavefunctions are assembled in a matrix form, the resulting wavefunction satisfied the requirements of Pauli's exclusion principle. This came to be known as the 'Slater determinant'. The Slater determinant for an N electron system can be written as follows:

$$\left| \Psi\left(\vec{r}_1,\vec{r}_2,\ldots,\vec{r}_N\right) \right\rangle = \frac{1}{\sqrt{N!}} \begin{bmatrix} \psi_1\left(\vec{r}_1\right) & \psi_2\left(\vec{r}_1\right) & \cdots & \psi_N\left(\vec{r}_1\right) \\ \psi_1\left(\vec{r}_2\right) & \psi_2\left(\vec{r}_2\right) & \cdots & \psi_N\left(\vec{r}_2\right) \\ \vdots & \vdots & \ddots & \vdots \\ \psi_1\left(\vec{r}_N\right) & \psi_2\left(\vec{r}_N\right) & \cdots & \psi_N\left(\vec{r}_N\right) \end{bmatrix} \quad (2.4)$$

where $\psi_i\left(\vec{r}_j\right)$ are the single electron wavefunctions.

Further simplification of the above equations was performed under the assumption to account for the electron-electron interaction. It was assumed that every electron will experience only a mean-field due to the rest of the electrons in the system, this gives rise to the simplification of the many electron Hamiltonian in equation (2.2) to a single electron Fock operator given by,

$$f\left(\vec{r}_i\right) = -\frac{1}{2}\nabla_i^2 - \sum_K \frac{Z_K}{\left|\vec{r}_i - \vec{R}_K\right|} + V^{HF}\left(\vec{r}_i\right) \quad (2.5)$$

18

where $f(\vec{r}_i)$ is the Fock operator, and V^{HF} is the mean field experienced by an electron. The potential V^{HF} is depedent on the other electrons all the single electron equations are essentially coupled and have to be solved numerically in a self-consistent manner. This iterative procedure has to be carried out until the wavefunction and the mean fields are self-consistent. This forms the basis of the Hartree-Fock method.

Hartree-Fock method is essentially a variational formulation, in which the trial wavefunction (basis set) is chosen that serves as the starting point for further optimization. From variational theorem, we know that the any trial wavefunction will estimate the energy higher or equal to that of the true ground state, Hartree-Fock provide an upper limit of the expected ground state energy. The best possible solution (wavefunction) can be achieved from a trial wavefunction by varying parameters until a minimum energy is obtained. The energy of the system can be expressed as,

$$E(\Psi) = \frac{\left\langle \Psi \left| \hat{H} \right| \Psi \right\rangle}{\left\langle \Psi | \Psi \right\rangle} \tag{2.6}$$

where, $\langle \ \rangle$ denoted the expectation of the operator.

A notable accomplishment of Hartree-Fock method is it implements exact exchange interaction. However, it suffers a major drawback, which is the complete absence of electron correlation which is a consequence of the use of the mean field approximation

to account for electron-electron Coulombic interaction. Many methods were proposed to overcome this drawback and can be collectively categorized as Post Hartree-Fock methods.

2.4 POST HARTREE-FOCK METHOD

It was realized that the absence of the electron correlation can allow two electrons to get extremely close to each other without a penalty to the overall energy of the system. One of the primary objectives of the post Hartree-Fock methods is to account for the electron correlation that is implemented as an average repulsion in the Hartree-Fock (HF) method. Many ideas were put forth for this purpose and a few of the widely used methods will be discussed in brief in this section.

A. Configuration Interaction (CI)

In order to account for the electron correlation in the HF framework, CI uses a sum of Slater determinant as opposed a single determinant used in HF.

$$\left| \Psi \right\rangle = c_0 \left| \Psi_0 \right\rangle + \sum_{r,a} c_a^r \left| \Psi_a^r \right\rangle + \sum_{r<s,a<b} c_{ab}^{rs} \left| \Psi_{ab}^{rs} \right\rangle + \dots (2.7)$$

where $\left| \Psi_a^r \right\rangle$ is formed by replacing the spin-orbital a by r in the Slater determinant $\left| \Psi_0 \right\rangle$. These additional determinants are also known as the excitations from the reference HF Slater determinant. Each of these additional determinants in equation

20

(2.7) are known as "configurations", therefore the method is termed as "configuration interaction". The strength of CI lies in its general form that can be extended to excited states of a given system. However, this method is computationally very exhaustive rendering its application restricted to very small systems. If the expansion includes all possible types of configurations are employed, then it is known as "Full CI". Many variations and improvements are developed for CI and are used in specific cases; however they are built on a common principle.

B. Møller-Plesset Perturbation (MP) Theory

MP treats the exact Hamiltonian of a system that includes electron correlation as the sum of the HF Hamiltonian and a small perturbation to it. It can be written as,

$$\hat{H} = \hat{H}_0 + \lambda \hat{H}'$$
(2.8)

where λ is an arbitrary parameter and $\hat{H}, \hat{H}_0, \hat{H}'$ are the exact, unperturbed and perturbation Hamiltonian. The corrections are obtained through the application of Rayleigh- Schrödinger perturbation theory. These corrections are added to the HF energies to obtain exact energies that include electron correlation.

C. Coupled Cluster (CC)

CC also utilizes multiple Slater determinants for account for the electron correlation. Unlike CI, CC relies on an exponential ansatz, to write the exact wavefunction as follows:

$$\left|\Psi\right\rangle = e^{\hat{T}}\left|\Psi_0\right\rangle \qquad (2.9)$$

Where $\hat{T}$ is an excitation operator or the cluster operator, that produces excited Slater determinant, thus making the exact $\left|\Psi\right\rangle$ a linear combination of the HF wavefunction ($\left|\Psi_0\right\rangle$). The exponential term can be expanded in terms of Taylor's series to improve on the accuracy of the calculation. Inclusion of higher order terms however, comes with a huge computational cost. Also, variations of the CC have been proposed.

2.5   DENSITY FUNCTIONAL THEORY (DFT)

In 1927, immediately after Schrödinger proposed his wave equation, Thomas and Fermi developed a model to approximate the electron distribution in an atom. The model was proposed for a non-interacting uniform electron gas in phase space. This conceptual leap reduced the 3N degrees of freedom of a many body problem to 3, significantly reducing the order of complexity of the technique. They have shown that the kinetic energy of a many body system can be expressed a functional of the number density of electrons,

$$T_{TF}\left[n(r)\right] = C_F \int n^{5/3}(r)d^3r \qquad (2.10)$$

where T_{TF} is the kinetic energy, $n(r)$ is the density of electrons and C_F is a constant that depends on the Fermi energy. Coulombic interactions were implemented from classical

terms in the Thomas-Fermi model. Corrections to the kinetic energy functional were proposed by Weizsäcker in 1935,

$$T\left[n(r)\right] = C_F \int n^{5/3}(r)\,d^3r + \frac{1}{8}\frac{\hbar^2}{m}\int \frac{\left|\nabla n(r)\right|^2}{n(r)}\,dr \quad (2.11)$$

A. Hohenberg-Kohn Theorems

The true foundations of the DFT can be dated back to Hohenberg-Kohn theorems proposed by Pierre Hohenberg and Walter Kohn in 1964,

Theorem I: *"The external potential $V_{ext}(\vec{r})$, and hence the total energy, is a unique functional of the electron density $n(\vec{r})$."*[22]

$$E\left[n(\vec{r})\right] = \hat{F}\left[n(\vec{r})\right] + \int n(\vec{r})\hat{V}_{ext}(\vec{r})\,d^3r \quad (2.12)$$

where, $\hat{F}\left[n(\vec{r})\right]$ is a functional of $n(\vec{r})$ only, and $E\left[n(\vec{r})\right]$ is the energy of the system. And $\hat{F}\left[n(\vec{r})\right]$ in equation (2.12) can be written as,

$$\hat{F}\left[n(\vec{r})\right] = \hat{T} + \hat{V}_{ee} \quad (2.13)$$

where, $\hat{T}$ is the kinetic energy and $\hat{V}_{ee}$ is the electron-electron potential.

Theorem II: *"The ground state energy can be obtained variationally: the density that minimises the total energy is the exact ground state density."*[22]

As a consequence of equation (2.12), we can write,

$$E\left[n(\vec{r})\right] = \left\langle \Psi_0\left[n(\vec{r})\right]\middle|\hat{H}\middle|\Psi_0\left[n(\vec{r})\right]\right\rangle \quad (2.14)$$

23

B. Kohn-Sham Approach

Although, Hohenberg-Kohn theorems provide a firm footing for DFT, it does not offer a practical way for solution to the many body problem. The Kohn-Sham formulation transforms a real fully interacting system with a fictitious non-interacting system with an effective potential that accounts for the real interactions. We can rewrite the Hohenberg-Kohn theorem with the constraint on number of electrons as follows,

$$\delta\left[\hat{F}\left[n(\vec{r})\right]+\int n(\vec{r})V_{ext}(\vec{r})d\vec{r}-\mu\left(\int n(\vec{r})d\vec{r}-N\right)\right]=0$$

where,

$$\mu=\frac{\delta\hat{F}\left[n(\vec{r})\right]}{\delta n(\vec{r})}+V_{ext}(\vec{r})\quad a\;n\;d\hat{F}\left[n(\vec{r})\right]=T\left[n(\vec{r})\right]+E_H\left[n(\vec{r})\right]+E_{XC}\left[n(\vec{r})\right]$$

$$E_H\left[n(\vec{r})\right]=\frac{1}{2}\iint\frac{n(\vec{r})n(\vec{r}')}{\left|\vec{r}-\vec{r}'\right|}d\vec{r}d\vec{r}'\quad and\quad \mu=\frac{\delta T\left[n(\vec{r})\right]}{\delta n(\vec{r})}+V_{KS}\left[n(\vec{r})\right]$$

$$V_{KS}\left[n(\vec{r})\right]=V_{ext}\left[n(\vec{r})\right]+V_H\left[n(\vec{r})\right]+V_{XC}\left[n(\vec{r})\right]$$

Also,

$$V_H\left[n(\vec{r})\right]=\frac{\delta E_H\left[n(\vec{r})\right]}{\delta n(\vec{r})}=\int\frac{n(\vec{r})}{\left|\vec{r}-\vec{r}'\right|}d\vec{r}'\quad and\quad V_H\left[n(\vec{r})\right]=\frac{\delta E_H\left[n(\vec{r})\right]}{\delta n(\vec{r})}$$

(2.15)

Assuming a non-interacting electron gas the wavefunction Ψ_{KS} can be written as,

$$\Psi_{KS}=\frac{1}{\sqrt{N!}}\det\left[\psi_1(\vec{r}_1)\psi_2(\vec{r}_2)\psi_3(\vec{r}_3)\ldots\psi_N(\vec{r}_N)\right]\quad(2.16)$$

Ground state density can be obtained by solving, N single electron Schrödinger equations,

$$\left[-\frac{1}{2}\nabla^2 + V_{KS}\left(\vec{r}\right)\right]\psi_i\left(\vec{r}\right) = \varepsilon_i\psi_i\left(\vec{r}\right) \qquad (2.17)$$

where, ε_i is a lagrange multiplier that ensures orthonormality of single electron wavefunctions $\psi_i\left(\vec{r}\right)$, the density is constructed from $\psi_i\left(\vec{r}\right)$ as,

$$n\left(\vec{r}\right) = \sum_i \left|\psi_i\left(\vec{r}\right)\right|^2 \qquad (2.18)$$

The above substitution into Schrödinger equations will lead to solution for energy and electron wavefunction but $E_{XC}\left[n\left(\vec{r}\right)\right]$ is unknown at this point. The exact form of the exchange-correlation are unknown, so with the aid of approximation one can attempt to solve the equation (2.17). The following sections will deal with some of the widely used approximations in DFT.

C. *Local Density Approximation (LDA)*

LDA is the simplest approximation that works well for solid systems, it was proposed by Hohenberg and Kohn. The exchange-correlation (E_{XC}) is approximated from an equivalent homogenous electron gas with a density $n\left(\vec{r}\right)$. The exchange was proposed by Dirac for Thomas-Fermi model and the correlation is calculated from interpolation of known extremes of high and low density values obtained from quantum monte carlo calculations. E_{XC} is given by,

$$E_{XC}^{LDA}\left[n(\vec{r})\right]=\int n(\vec{r})\varepsilon_{xc}^{hom}\left[n(\vec{r})\right]d\vec{r}$$

where, (2.19)

$$\varepsilon_{X}\left[n(\vec{r})\right]=-\frac{3}{4}\left(\frac{9}{4\pi^{2}}\right)^{1/3}\frac{1}{r_{s}}$$

where, ε_{XC}^{hom} is the exchange-correlation for a homogenous gas, and r_{s} is the wigner-seitz radius and $\varepsilon_{x}\left[n(\vec{r})\right]$ is the exact exchange as given by Dirac.

D. Generalized Gradient Approximation (GGA)

GGA is an improvement over LDA and assumes that E_{XC} depends on density and its gradient, an analytic term the correction or the gradient term is also known as an enhancement factor. Equation (2.20) shows the functional form of GGA and as an example the exchange term in PW91 is also shown,

$$E_{XC}^{GGA}\left[n(\vec{r})\right]=\int n(\vec{r})\varepsilon_{xc}^{hom}\left[n(\vec{r})\right]F_{XC}\left[n(\vec{r}),\nabla n(\vec{r})\right]d\vec{r}$$

where, (2.20)

$$F_{x}^{PW91}\left[n(\vec{r})\right]=\frac{1+0.19645s\sinh\left(7.7956s\right)+\left(0.2743-0.15084e^{-100s^{2}}\right)s^{2}}{1+0.19645c\sinh^{-1}\left(7.7956s\right)+0.004s^{4}}$$

Electronic Properties of Zig-Zag

Carbon Nanotubes

Using a first-principles gradient corrected density functional approach, we present a comprehensive study of the geometry and energy band gap in moderate-gap zig-zag semi-conducting $(n,0)$ carbon nanotubes (CNT) to resolve some of the conflicting findings. Up to (8,0), curvature induced distortions leads to a strong deviation in energy band gap (E_g) derived from a simple zone folding picture of grapheme based on tight binding calculation. From (10,0) onwards, the gap dependence on the radius of the tube can be explained surprisingly well with the zone-folding scheme of the graphene bandstructure, if the trigonal shape of the equi-energy lines around the **K**-point is properly taken into account. Our extensive first principle calculations confirm that the $(n,0)$ CNTs fall into two distinct classes depending upon n mod 3 equal to 1 (smaller band gaps) or 2 (larger gaps). The amplitude of the gap oscillations, arising from σ - π mixing, decreases from $n = 10$ to $n = 17$. From $n = 19$ onwards, the gap follows a $\dfrac{1}{d}$ behavior predicted from the simple tight binding π – model with decaying amplitude. The effect of longitudinal strain on the band gap further confirms the existence of two

distinct classes: for n mod 3 = 1 or 2, changing E_g by ~100 meV for 1% strain in each case.

3.1   INTRODUCTION

A Carbon nanotube (CNT) is a one dimensional (1-D) nanostructured material, which has been the focal point of research over the past decade for intriguing applications ranging from nanoelectronics to chemical and biological sensors. The geometry of the carbon nanotube is uniquely described by a chiral vector ($\vec{C}$): $\vec{C} = n\,\vec{a} + m\,\vec{b}$, denoted by a pair of indices (n, m) that connect the two crystallographically equivalent sites on the graphene sheet. Soon after their discovery and characterization [5], the potential of this tubular structure was realized by theoretical work [23-27] , which showed that the single wall CNT can be categorized into three types; metallic, small gap semiconducting, and moderate gap semiconducting based on their chirality's. It was proposed that the single wall CNT would exhibit metallic character if $\left(\dfrac{n-m}{3}\right)$ is an integer, and a moderate gap semiconductor in all other cases. Furthermore, these early tight-binding based theoretical calculations also predicted that the E_g in a moderate gap semiconducting carbon nanotube (SCNT) is inversely proportional to its diameter [28] and monotonically decreases with the increase of diameter of the tube. This unique dependence of electronic properties of CNT on their diameter and chirality's, which has spawned great interest in this material, was confirmed later by the pioneering

28

experimental work that measured electronic properties of CNT [29-32] . These experiments used scanning tunneling microscope to probe the explicit dependence of chirality's and diameter on the electronic properties reported by theory. Both the experiments confirmed the earlier theoretical predictions with accuracy of ± 0.05 nm in measured diameter, and ± 0.3 eV in measured E_g. It should be noted that the band gap in SCNT is expected to be of the order of ~ 0.5 eV.

However, over the years, conflicting relationships have been reported on the exact dependence of the E_g of the SCNT on its diameter. Previous conclusions about monotonic $\dfrac{1}{d}$ dependence law in SCNT have been corrected. For smaller n the trigonal shape of the equi-energy lines around the **K**-point of the graphene Brillouin zone (BZ) ("trigonal warping" [33]) needs to be taken into account. Yorikawa *et. al.* [34] have shown that a third order Taylor expansion of the energy dispersion relation around **K**-point leads to the equation for E_g, which depends on the chirality of the tubes (more general analytic expression have been given later by Reich *et. al.* [35]). In later papers, an empirical parameter (γ) was used to account for the *curvature* effect which changes not only the *overlap* between π orbitals but causes *mixing* between π and σ orbitals [36]. For a (n,0) SCNT, the energy band gap is given by:

$$E_g = \frac{2\pi}{3}\gamma_0\left[\frac{1}{n} + \left(-1\right)^{n \bmod 3}\gamma\frac{2\pi}{\sqrt{3}}\frac{1}{n^2}\right] \qquad (3.1)$$

where, E_g is the energy band gap, γ_0 (=2.53eV) is a parameter, n is the chiral index of a SCNT.

Tight binding predictions formed the basis for identification of chirality's of SCNT and interpretation of experimental results [37]. Spectrofluorimetric measurements were used in conjunction with resonant Raman data [37] to show that SCNT follow two distinct trends depending on $(n-m)$ mod 3 equal to 1 or 2 respectively. Following the experimental work, a first principle generalized gradient approximation study reported significant deviations from the simple tight binding predictions for tubes with radius smaller than 3.5 Å (n= 7,8), but confirmed results for larger n. The band gap for n mod 3 equal 2 class is higher than the other class [38]. D'yachkov and Hermann [39] used a linear augmented cylindrical wave (LACW) method to show that the band gap in SCNTs is oscillatory in nature depending on $(n-m)$ mod 3 equal to 1 or 2 but reached opposite conclusions for the two classes: the n mod 3 =1 class has larger gaps than the n mod3 = 2. Fantini $et.$ $al.$ [40, 41] determined the electronic transistion energies of several nanotubes with different chiralities using stokes and anti-stokes dependence of resonant Raman spectroscopy, and confirmed the existence of two classes of SCNT, depending on $(2n+m)$ mod 3 equal to 1 or 2 respectively. Telg $et.$ $al.$ [42, 43] reported the evidence of two classes of SCNT based on $(n-m)$ mod 3; they interpreted their results based on three nearest neighbor tight binding model proposed by Reich et $al.$ [44]. Again, very recently, Kozinsky and Marzari [45], have reported a different trend

in the band gap for SCNTs. They have used first-principles plane wave based density functional approach and found a monotonic decrease in E_g with the increase of diameter (from (10,0) to (17,0)) as suggested by early tight-binding work that did not account for the trigonal shape of equi-energy lines around **K**-point, in contrast to the non-monotonic variation of E_g with diameter reported by several groups in the last few years [35, 38, 39]. Thus far, no consistent effort is made to resolve this important issue that is central to the assignment of chirality's of CNT.

3.2   METHODOLOGY

In this study, we have used a consistent and systematic approach to address this controversial picture. Using exhaustive ab-initio density functional computations for SCNTs up to (41,0), we show that the energy band gaps in zig-zag SCNTs indeed deviate from a simple $\dfrac{1}{d}$ dependence to the diameter. Our calculations are performed using periodic density functional method, which involves generalized gradient (GGA) approximation for the exchange and correlation within the framework of Perdew-Wang 91 formalism [46, 47]. We have used the Vienna *ab-initi*o Simulation Package (VASP) [48] to carry out the calculations. To construct the 1-dimensional (*n*,0) nanotube structure within the periodic approach, we placed the one unit cell of the (*n*,0) in a tetragonal lattice with the tube parallel to the z-axis. The longitudinal translational vector (along z- axis) was varied from 4.25 Å to 4.28 Å to find the optimal z-translation

based on minimal total energy. The other two sides of the unit cell are chosen in such a way that the inter-wall distance between the tubes for different diameter is kept fixed at ~11 Å. This large inter-wall separation is used to ensure negligible interaction between the nanotube and its images along x, and y-direction. The geometries of the moderate gap SCNT are found to be sensitive to the number of *k*-points used to sample the Brillouin Zone (BZ), we have used 1x1x7 *k*-point mesh (Monkhorst-Pack) for optimization purposes. The minimum force criterion of 0.01 eV/Å is used for individual atom during the structural relaxation. The convergence threshold for energy is taken to be 10^{-6} eV. Wehave tested the convergence for E_g; for example, in the case of (8,0) SCNT, a 1x1x1 *k*-point (1 irreducible *k*-point) predicts a 0.7242 eV band gap, a 1x1x7 *k*-point (4 irreducible *k*-points) mesh yielded 0.591 eV for the band gap, which is changed to 0.5904 eV with 1x1x11 *k*-point mesh (7 irreducible *k*-points). The plane wave cutoff is taken to be 286.74 eV and kept fixed for all SCNT with different diameters.

3.3   RESULTS AND DISCUSSIONS

First we comment on the stability of these SCNT, we have calculated the curvature energy per atom for optimized SCNT. Cohesive energy per atom is calculated as,

$$E_c = \frac{\left(E_{NT} - E_{NT}^{\infty}\right)}{N}$$ where E_{NT} is energy of nanotube; E_{NT}^{∞} is the energy of a CNT

with ∞ diameter (graphene), and N is the total number of atoms in the nanotube. The

curvature energy is found to increase with the increase in diameter, saturating at ~ 25 Å

diameter of the SCNT. These results are consistent with previous reported values

obtained from *ab-initio* calculations as a measure of the stability of nanotubes [38].

Figure 3.1 shows the results for Kohn-Sham direct energy band gap as a function of

their diameter indicating deviation from a simple monotonic decrease in band gap with

increase in diameter of the SCNT. Up to (8,0), the strong curvature distortions change

the simple picture derived from the properties of graphene. From (10,0) on, the gap

dependence on the radius of the tube can be explained surprisingly well with the simple

relation derived from tight binding calculations and the zone-folding of the graphene

that accounts for the trigonal shape of the equi-energy lines around the **K**-point. Our

first-principles calculations confirm that the (n,0) SCNT fall into two classes depending

upon n mod 3 equal to 1 (smaller band gaps) or 2 (larger gaps). The amplitude of the

gap oscillations, enhanced through the curvature induced σ - π mixing, decreases from

(10,0) to (17,0). From $n = 19$ onwards, corresponding to a radius of ~15Å, the gap's *d*-

dependence roughly follows the $\dfrac{1}{d}$ behavior predicted from the simple tight binding π –

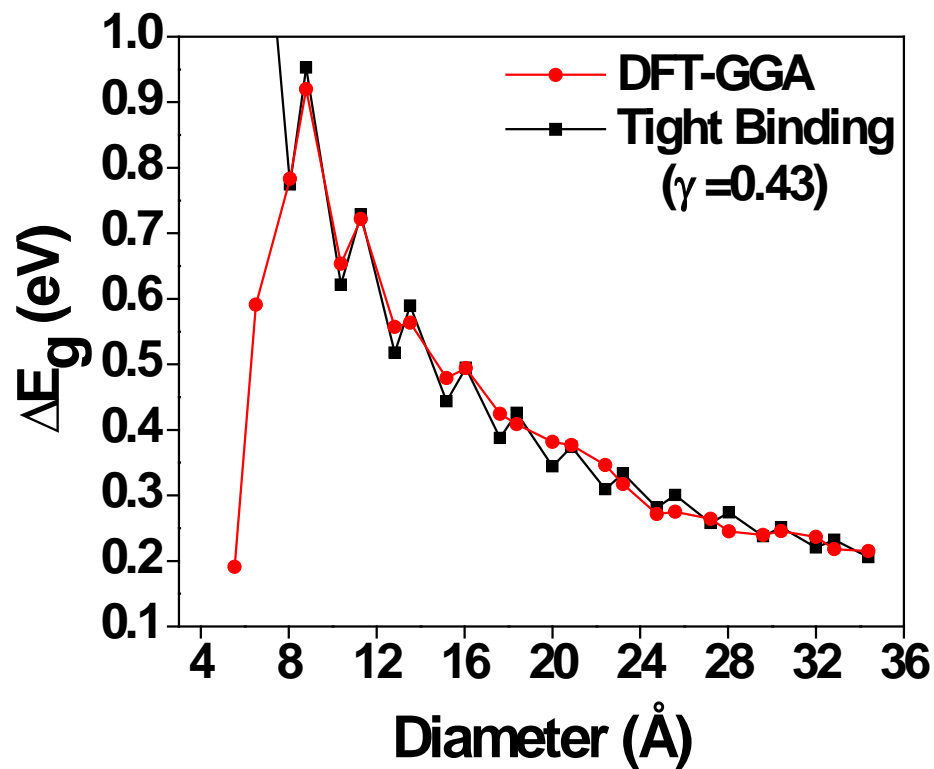model with decaying amplitude of oscillations.

Figure 3.1 Energy band gap (E_g) as a function of the diameter of the SCNT, the circles show the predictions from density functional theory within GGA and the squares represent predictions from a tight binding model with a parameter $\gamma = 0.43$

A distinction in the trends of the two classes of SCNT is observed based on the values of n mod 3. Within each class of SCNT the band gap decreases monotonically with increasing diameter beyond the initial curvature dominated region ($n < 8$). Figure 3.2 shows the energy band structures for three representative CNT's. This figure confirms the band gap of the SCNT's being oscillatory. Each energy band around the Fermi level in the Figure 3.2 is doubly degenerate.

For smaller n (10 to 17) the trigonal shape of the equi-energy lines around the **K**-point of the graphene BZ ("trigonal warping" [33]) needs to be taken into account. Yorikawa *et. al.* [34] have shown that a third order Taylor expansion of the energy dispersion relation around **K**-point leads to the equation for energy band gap, which depends on the chirality of the tubes (more general analytic expressions have been given later by Reich *et. al.* [35]) :

$$
\begin{aligned}
E_g \quad &= \gamma_0 d_{C-C} \left[\frac{1}{r} + (-1)^p \frac{1}{12} \cos(\theta) \frac{1}{r^2} \right] \\
&= \frac{2\pi}{3} \gamma_0 \left[\frac{1}{n} + (-1)^p \frac{1}{12} \cos(\theta) \frac{2\pi}{3} \frac{1}{n^2} \right]
\end{aligned}
\qquad (3.2)
$$

where, E_g is the energy band gap, γ_0 is a parameter, d_{C-C} is the carbon-carbon bond length, n is the chiral index of a SCNT, θ is the chiral angle ($\theta=0°$ for zig-zag SCNT) and $p = n$ mod 3.
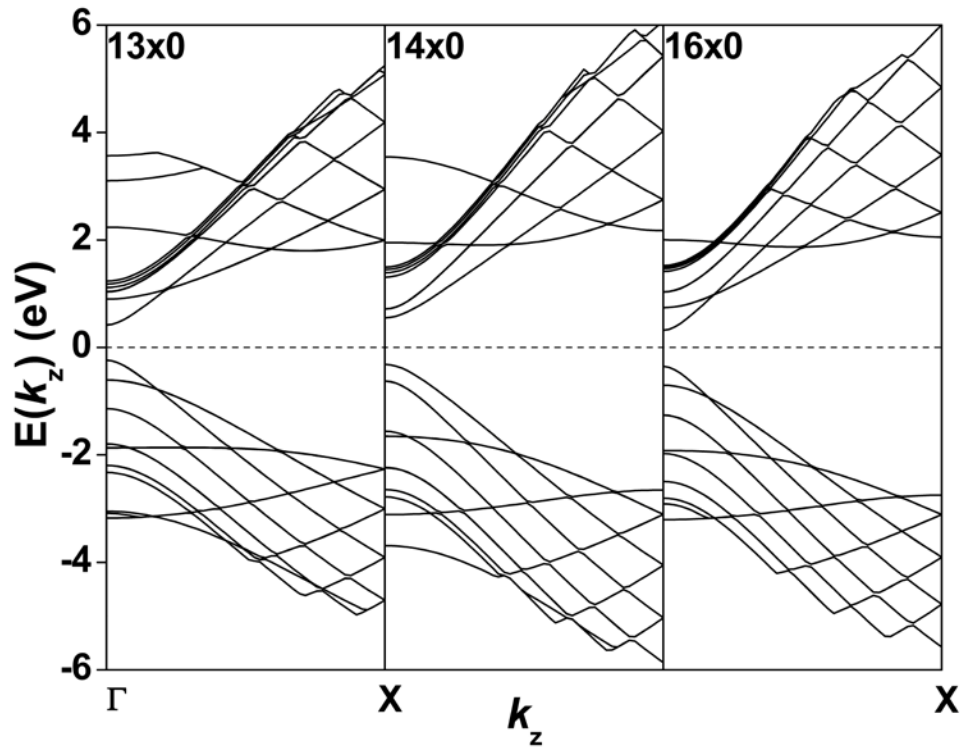
Figure 3.2 Energy band structure of three representative SCNT (13,0), (14,0) and (16,0) respectively. The dotted line at zero represents the Fermi energy level

For zig-zag tubes ($\cos\theta = 1$), maximum trigonal warping effect is expected. In the presence of warping, equation (3.2) predicts that the energy band gap for "mod 1" class is reduced (k_{vic}, the point in the projected BZ of grapheme closest to **K**-point which determines the gap in CNT, approaches **K** from the **M**-point outside the first BZ). In case of "mod 2" class the gap becomes larger (k_{vic} approaches **K** from **Γ**-point). This same effect, of course, explains the splitting of the van Hove singularities in the n mod $3 = 0$ or metallic cases: k_{vic} coincides with **K**-point and leads to the metallic state; the energies at $k_{vic} \pm = \dfrac{4\pi}{3a_0} \pm \dfrac{2\pi}{na_0}$ are no longer the same and the corresponding van Hove singularities in the density of states split [33]. In later papers, it was suggested to replace $\dfrac{1}{12}$ in Equation (3.3) by a parameter γ [36]. A larger γ would increase the effect of gap reduction (mod 1 class) and gap increase (mod 2 class), thus defining the amplitude of these gap oscillations:

$$E_g = \frac{2\pi}{3}\gamma_0\left[\frac{1}{n} + (-1)^{n \bmod 3}\gamma\frac{2\pi}{\sqrt{3}}\frac{1}{n^2}\right] \qquad (3.3)$$

where γ would empirically take into account the *curvature* effect which changes not only the *overlap* between π orbitals but causes *mixing* between π and σ orbitals.

Conduction Band

(13,0)   **(14,0)**   **(16,0)**
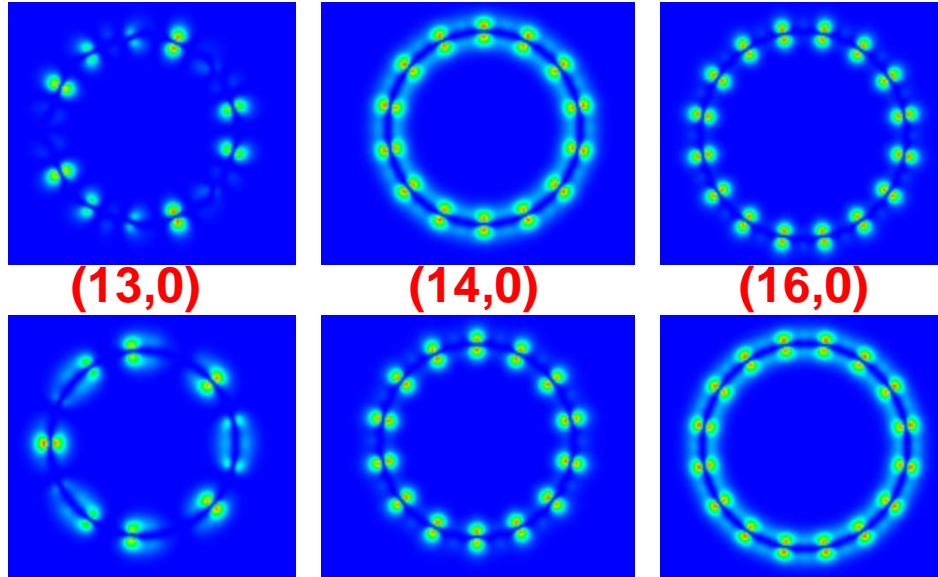
Valence Band

Figure 3.3 Band decomposed charge density at the Γ-point for (13,0), (14,0) and (16,0)
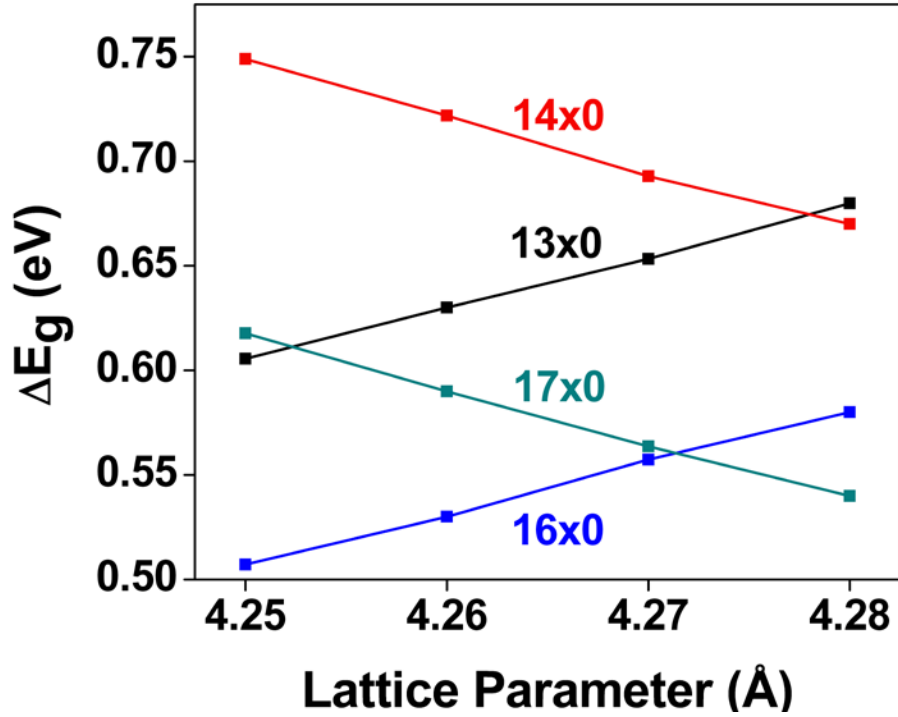
Figure 3.4 Energy band gap (E_g) as a function of the lattice parameter along the longitudinal axis (z-axis) of the CNT

Yorikawa *et. al.* [36] showed that γ is determined by $\left|\dfrac{V_{pp\pi}}{V_{pp\sigma}}\right|$ alone (where $V_{pp\pi}$ and $V_{pp\sigma}$ are tight bindings parameters for π and σ bonding orbitals respectively), independent of the other tight binding parameters (see Figure 3.2 in [36]), and that the mixing between σ and π orbitals increases γ to ~ 0.43 for $\left|\dfrac{V_{pp\pi}}{V_{pp\sigma}}\right| = 3$ from its π-orbital-only graphene

value of $\dfrac{1}{12}$ (= 0.08333) and thus enhances the chirality dependence of the gap and the amplitude of the gap oscillations for between the "mod 1" and "mod 2" semiconductors. The predictions from this model are also plotted in Figure 3.1.

The energy bands around the Fermi energy are primarily of π and π^* in nature for the valence and conduction band respectively. We analyzed the band decomposed charge density at the Γ-point for the three SCNT's (Figure 3.3). It can be seen from the Figure 3.3 that the valence band in (13,0) and (16,0) show a bonding character with electron cloud smeared between atoms along the circumference which is more evident in (16,0). The conduction band in this class (n mod 3 = 1) shows more of an anti-bonding character with electron clouds highly localized around the atoms. In case of (14,0) i.e. n mod 3 = 2 class show an opposite trend of localized electron cloud in the valence band and a more banding character in the conduction band.

We have varied the lattice parameter along the axis of the SCNT (z-axis) from 4.25Å to 4.28 Å, for all the SCNTs, to find the influence of longitudinal strain on the energy band gap (Figure 4). The band gap in the two different classes of SCNT found to exhibit opposite trends; the band gap for n mod 3 = 1 increases with increase in the z-axis translation. For n mod 3=2, the band gap found to decrease with the increase in z-translation. Again this confirms two classes of SCNT. Furthermore, it also suggests an optimal z-translation is crucial for obtaining correct feature of the band gap oscillation.

We believe the absence of band gap oscillation reported by Kozinsky and Marzari [45] could be due to this effect, which might have been overlooked during structural optimization.

A study by Capaz *et. al.* utilizing frozen-phonon scheme to understand the temperature dependence of band gap in SCNT through electron-phonon coupling also reported the existence of two classes of SCNT [49]. This study has shown that the two classes arise from the difference in sign of the e-p coupling associated with low-energy optical phonons. The *n* mod 3 = 2 class of SCNT exhibits a non-monotonic relationship of the energy band gap (E_g) with increasing temperature. The existence of two classes of SCNT was also inferred from the electron-phonon (e-p) coupling matrix elements that indicate sign alteration [50] between the two classes. They have shown that the e-p coupling is stronger for zig-zag than for armchair nanotubes. A recent experimental study utilizing electron diffraction with Rayleigh scattering techniques to measure electronic and optical properties of CNT confirms the two family of SCNT based on (*n-m*) mod 3 equal to 1 or 2 [51]. This study is the first experimental evidence of the distinct class behavior based on the n mod 3 values unlike the previous experimental work which relied on theoretical work for interpretation of data [51].

We have varied the lattice parameter along the axis of the SCNT from 4.25Å to 4.28 Å, to find the influence of longitudinal strain on the E_g (Fig. 3.4). The E_g in the two different classes of SCNT found to exhibit opposite trends; the band gap for *n* mod 3 =

1 increases with increase in the z-axis translation. For $n \bmod 3=2$, the band gap is found to decrease with the increase in z-translation. Again this reinforces the existence of two distinct classes of SCNT. It also suggests an optimal z-translation is crucial for obtaining correct feature of the E_g. We found that the longitudinal strain changes band gap by ± 110 meV for 1% strain; for $n \bmod 3=1$, the gap increases, and for $n \bmod 3=2$, it decreases. These *ab-initio* results are in agreement with earlier tight binding predictions that report $\Delta E_g = \pm 3\gamma_0 (1+\nu)\sigma$, where σ is the fractional change in length along the strain axis and ν is the Poisson ratio of the material. For $\nu=0.2$ and $\gamma_0=3$eV, $\Delta E_g = 108$meV for $\sigma = 0.01$ (1% strain).

Table 3.1 summarizes the values reported in the literature for E_g for SCNT. The first row is the E_g calculated from the current study, which is in good agreement with the values reported for (7,0) to (14,0) of Ref. [38]; LDA result for (8,0) of Ref. [52]; (10,0) and (11,0) of Ref. [34, 36]. Also, our results match qualitatively for (10,0) to (14,0) of Ref. [23]. We believe the absence of band gap oscillation reported in Ref. [45] is a consequence of non-optimal z-translation leading to spurious strains in CNT. It should be noted that the trend in E_g obtained from a crude single *k*-point sampling of the BZ during structural optimization will yield persistent oscillations of E_g from $n=11$ onwards, as observed in Ref. [39]. The discrepancy between the current results and the tight binding values reported for (7,0) and (8,0) [23, 36, 52] can be attributed to the strong curvature effect that is not included in these tight-binding models . The experimental values in Table 3.1 are calculated from a π-electron model that does not

account for σ−π mixing. At smaller diameters, the subtle deviation in values from Ref. [29] is due to the use of π-electron model for diameter assignment that does not account for trigonal shape of the equi-energy lines around the **K**-point. We see better agreement with results at larger diameters from Ref. [30] as the influence of σ−π mixing is negligible in this regime. It was reported that a strong curvature poses great difficulty in accurate measurement of the chiral angel in Ref. [30] and could be responsible for a significant deviation in E_g for (11,0). A recent experimental study utilizing electron diffraction with Rayleigh scattering techniques to measure electronic and optical properties of CNT confirms the two family of SCNT based on (*n-m*) mod 3 equal to 1 or 2 [51].

3.4   SUMMARY

In summary, we have used *ab-initio* gradient corrected density functional computations to investigate the dependence of the energy band gap in zig-zag SCNT on the diameter of the tube. We confirm the existence of two classes of SCNT based on *n* mod 3 equal to 1 or 2. Within each class the band gap is found to decay monotonically with the increase of diameter. Up to (8,0), a strong curvature distortions lead to strong deviation from a simple picture derived from the properties of graphene. From (10,0) on, the gap dependence on the radius of the tube can be explained surprisingly well with a simple relation derived from early tight binding calculations and the zone-folding of the graphene bandstructure. If the trigonal shape of the equi-energy lines around the **K**-

point is properly taken into account, our extensive first principle calculations confirm that the zig-zag semi-conducting carbon nanotubes (n,0) fall into two classes depending upon n mod 3 equal to 1 (smaller band gaps) or 2 (larger gaps). The origin of strong oscillation arises from the alternating bonding and anti-bonding character of the valance bands between the two classes of SCNTs. We also found, the transition from semi-conducting to metallic behavior occurs at ~ (43,0), with a gap of ~0.15 eV. This allows us to set a new upper limit for the diameter of the SCNT to ~40 Å, beyond which we would not observe any single wall zig-zag SCNT.

Table 3.1 Energy band gap (Eg) as a function of the chirality of zig-zag SCNT. The first row under *ab-initio* presents the data from the current study obtained from DFT-GGA

n	7	8	10	11	13	14	16	17
Ab-initio								
E_g	0.19	0.59	0.78	0.92	0.65	0.72	0.56	0.56
Ref. [45]	0.48	0.57	0.91	0.77	0.72	0.63	0.61	0.53
Ref. [38] GGA	0.24	0.64	0.764	0.939	0.63	0.74	-	
Ref. [52] LDA	0.09	0.62	-	-	-	-	-	
Tight Binding								
Ref. [36]	1.11	1.33	0.87	0.96				
Ref. [52]	1.04	1.19	-	-	-	-	-	
Ref. [23]	1.0	1.22	0.86	0.89	0.69	0.7	-	
Experiment								
Ref. [29]			$0.9\pm0.0.05^a$	0.78 ± 0.07^a				
Ref. [30]				1.9 ± 0.05^b			0.5 ± 0.05^b	$*0.55\pm0.05^b$

[a] Data obtained from Figure 3 (c) of Ref. [29] $E_g = \dfrac{2\gamma_0 d_{C-C}}{d}$

[b] Data obtained from Table I of Ref. [30] for d=1.4Å and chiral angle 30º (zig-zag), E_g calculated similar to [a]

* Reported chiral angle 25º, with an accuracy of (~1º)

Origin of Metallic Behavior in Multiwall Carbon Nanotubes

Following the discovery of CNT many applications have been proposed for its use, each relied on its unique electrical and mechanical properties. However, based on the structure, in particular, the presence of multiple concentric rolled up graphene sheets can be used to classify the nanotubes as SWCNT or multi-wall CNT (MWCNT). Chapter 3 provides a detailed study on the nature of the electronic properties of single walled zig-zag semi conducting $(n,0)$ carbon nanotubes. It was found that the zig-zag $(n,0)$ SWCNTs can be classified based on n mod 3 value. They are metallic if n mod $3 = 0$ and semiconducting otherwise. Also, the single walled SCNT can be further classified into two classes based on upon n mod 3 equal to 1 (smaller band gaps) or 2 (larger gaps). But semiconducting behavior for MWCNT (more than 3 concentric tubes) has been seldom reported in previous studies.

4.1   METHODOLOGY

In this chapter, we report the results from extensive calculations of electronic properties of multiple wall CNTs. Using *ab-initio* density functional computations for various nanotubes, we show that the zig-zag MWCNT do not exhibit semiconducting behavior beyond three walls. Our calculations are performed using periodic density functional method, which involves generalized gradient (GGA) approximation for the exchange and correlation within the framework of Perdew-Wang 91 formalism [46, 47]. We have used the Vienna *ab-initi*o Simulation Package (VASP) [48] to carry out the calculations. To construct the 1-dimensional nanotube structure within the periodic approach, we placed the one unit cell of the concentric SWCNT in a tetragonal lattice with the tube parallel to the z-axis. It has been shown in previous studies that MWCNTs with intertube separation close to the interlayer separation in graphitic are more stable [53]. Some experiments have shown that different interlayer spacing is probable [54-56]; in the current study we restrict our study to MWCNT with separation close to ~ 3.5Å. The longitudinal translational vector (along z- axis) was varied from 4.25 Å to 4.28 Å to find the optimal z-translation based on minimal total energy. The other two sides of the unit cell were chosen in such a way that the inter-wall distance between the tubes for different diameter is kept fixed at ~11 Å. This large inter-wall separation is used to ensure negligible interaction between the nanotube and its images along x, and y-

direction. The minimum force criterion of 0.01 eV/Å is used for individual atom during the structural relaxation.

The convergence threshold for energy is taken to be 10^{-6} eV. We have tested the convergence for E_g; for example, in the case of (16;7,0) which represents (7,0) inside (16,0) double-walled CNT (DWCNT), a 1x1x1 k-point (1 irreducible k-point) predicts a 0.2069 eV band gap, a 1x1x5 k-point (3 irreducible k-points) mesh yielded 0.06 eV for the band gap, which is changed to 0.04 eV with 3x3x11 k-point mesh (16 irreducible k-points). The plane wave cutoff is taken to be 286.74 eV and kept fixed for all MWCNT with different diameters.

We have also tested the convergence with cohesive energy per atom for (16;7,0) and the results are plotted in Figure 4.1. It can be seen that a minimum of 3 irreducible k-points are required for accurate prediction in structure and related properties. As discussed in detail in Chapter 3, the single wall (n,0) CNT fall into two classes depending on the value of n mod 3 = 1 or 2. We have calculated the energy band gap for various combinations of (n,0) SWCNT for inner and outer wall of DWCNT. Figure 4.2 – 4.8 shows the energy band structure for various combinations of the SWCNT with different energy band gaps. Figure 4.2 and 4.3 show the band structure of DWCNT with (7,0) as the inner wall. A (7,0) is a semi-metallic SWCNT with Eg ~ 0.2eV, however, when it is the inner shell of a DWCNT leads to overall metallicity of the structure.
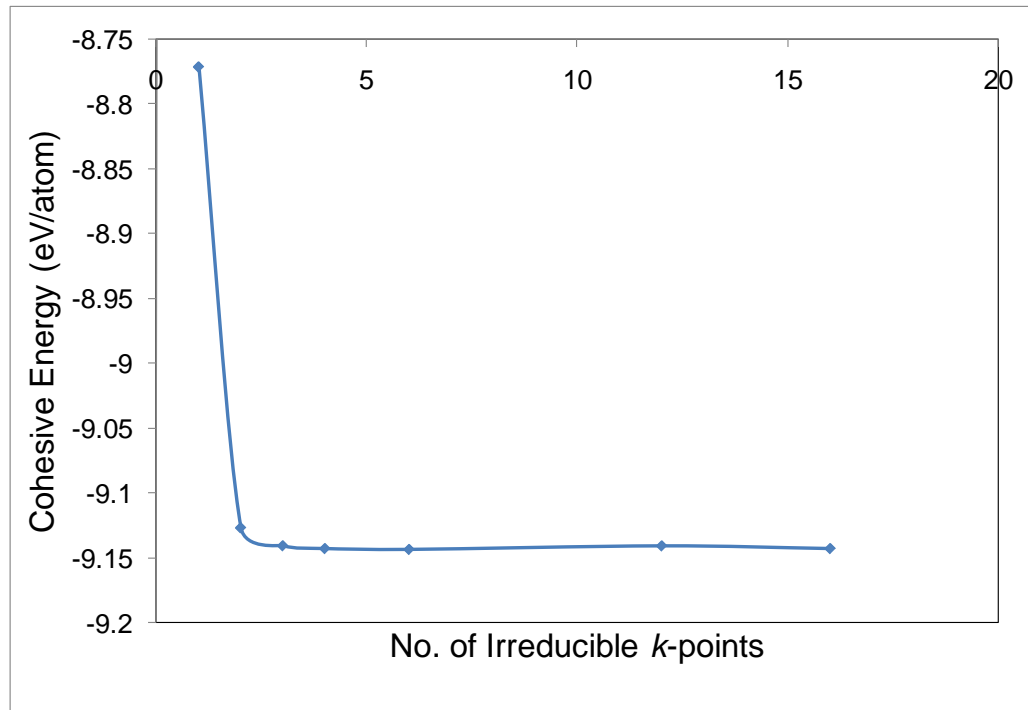
48

Figure 4.1 Cohesive energy per atom of (16;7,0) as a function of number of irreducible

k-points used in structural optimization

4.2   RESULTS AND DISCUSSIONS

This section presents the results obtained from electronic structure calculation of DWCNT and MWCNT for different combinations. As described in Chapter 3, the SWCNT can be semi-conducting, semi-metallic or metallic. Different SWCNT such as (7,0), (8,0), (10,0) and (11,0) were chosen as the inner wall for the current. For the outer wall, (16,0), (17,0), (19,0), (20,0) and (26x0) were considered. The SWCNT

combination for DWCNT MWCNT was chosen to keep the interwall distance between

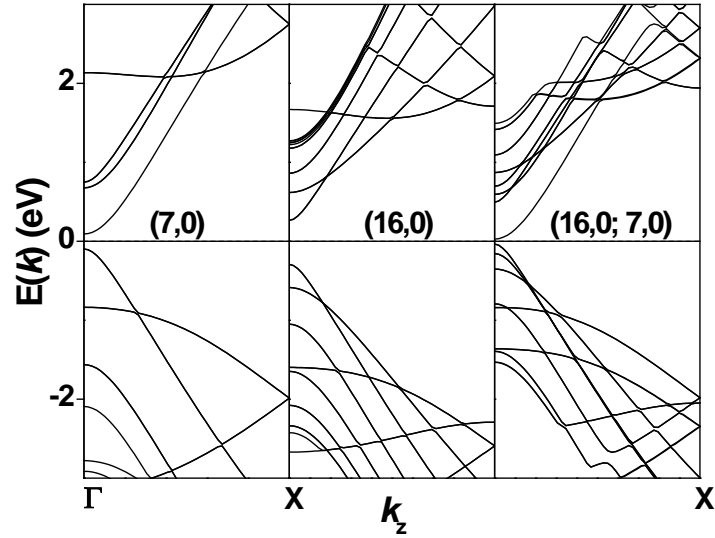the constituent shells close to the graphite interlayer distance.

Figure 4.2 Energy band structure of (7,0), (16,0) and (16;7,0) (left to right). The zero
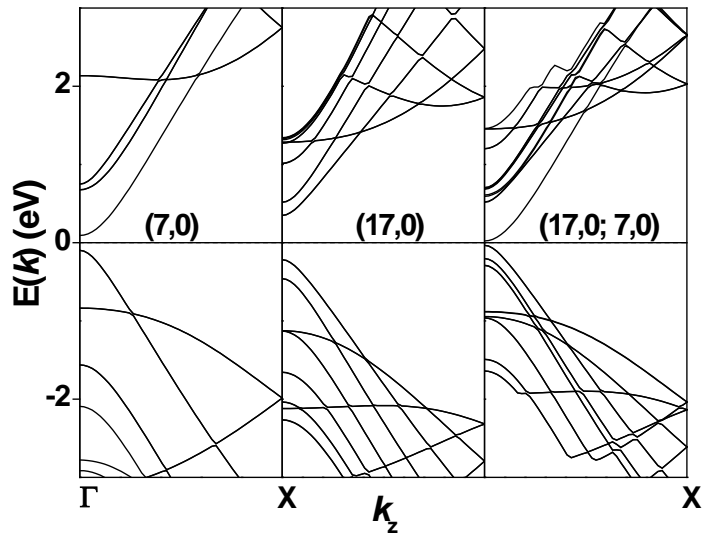represents the Fermi energy

Figure 4.3 Energy band structure of (7,0), (17,0) and (17;7,0) (left to right). The zero
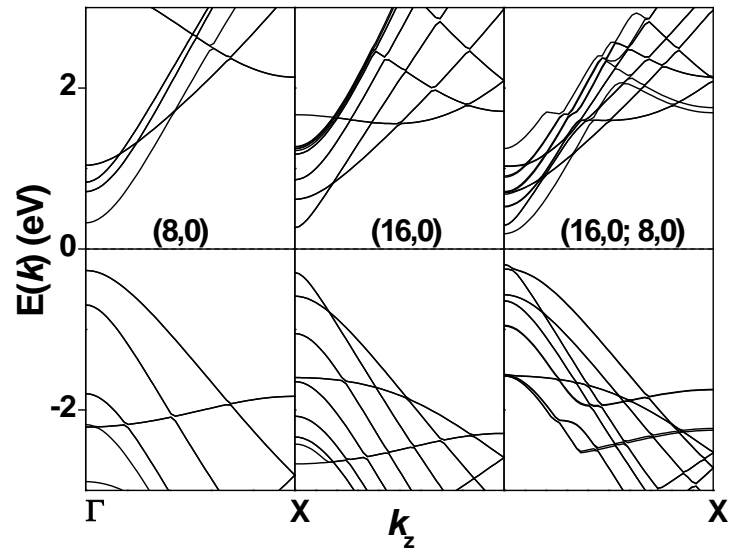represents the Fermi energy level.

Figure 4.4 Energy band structure of (8,0), (16,0) and (16;8,0) (left to right). The zero represents the Fermi energy level.
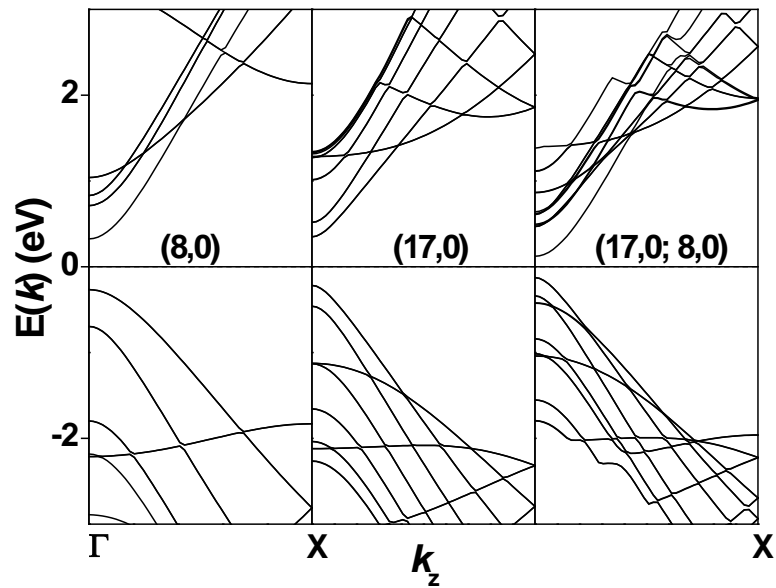

Figure 4.5 Energy band structure of (8,0), (17,0) and (17;8,0) (left to right). The zero represents the Fermi energy level.

Figure 4.4 and 4.5 show the band structure with (8,0) inner wall and (16,0) and (17,0) being the outer wall respectively. It has been shown in Chapter 3 that (8,0) has an energy band gap of ~0.6 eV and the outer wall CNT ~ 0.55 eV. Both (8,0) and (16,0) are semi-conducting CNT that have a definite energy band gap. However, the DWCNT with these SWCNT as the constituents has a band gap of ~0.4 eV, this suggests the possibility of interwall interactions that could be responsible for the reduction in the energy band gap that occurred as a consequence of adding concentric SWCNT to (8,0). In case of (17,0) as the outer wall the energy band gap was reduced to ~0.25eV; again suggesting the net band gap of the overall structure is lower than any of its constituents. Figure 4.6 – 4.9 show the band structure of different combinations of DWCNT constructed from (10,0), (11,0) as the inner tubes and (19,0), (20,0) as the outer tubes respectively.
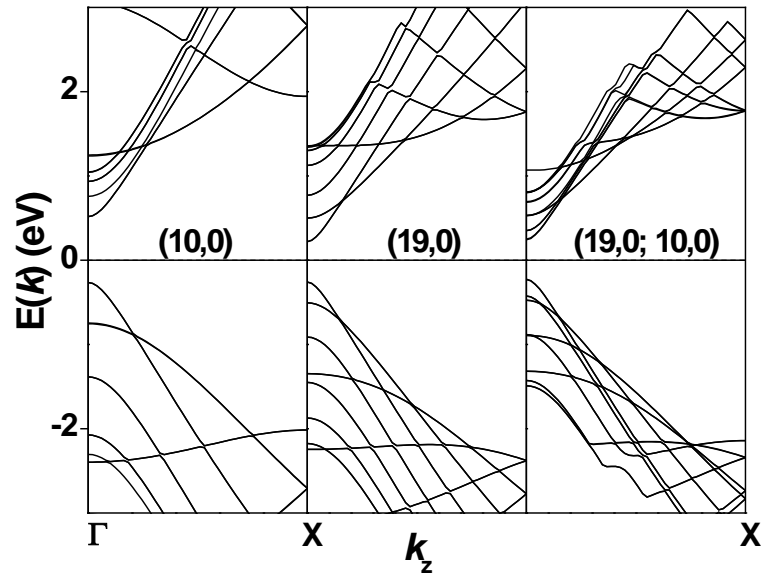
Figure 4.6 Energy band structure of (10,0), (19,0) and (19;10,0) (left to right). The zero represents the Fermi energy level.
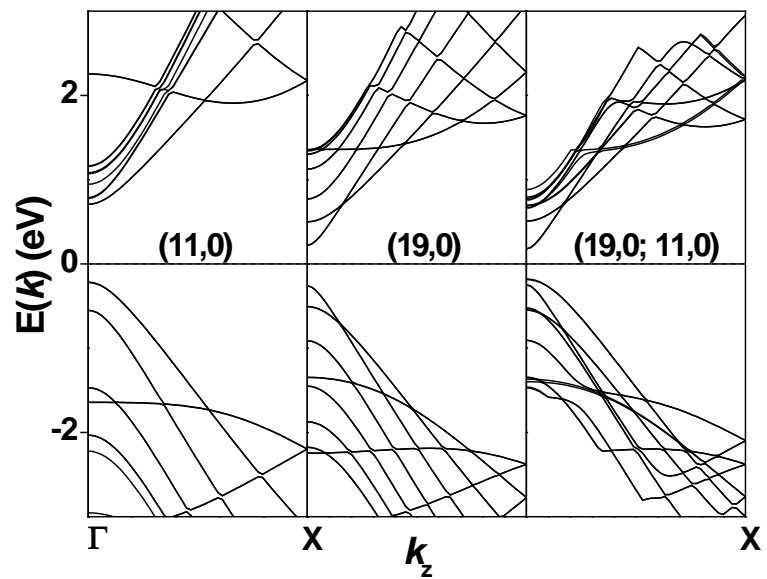

Figure 4.7 Energy band structure of (11,0), (19,0) and (19;11,0) (left to right). The zero represents the Fermi energy level.
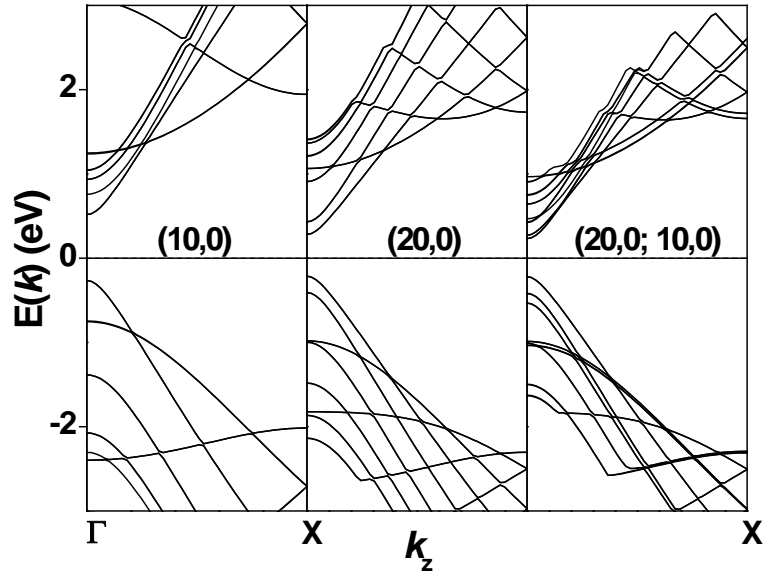
Figure 4.8 Energy band structure of (10,0), (20,0) and (20;10,0) (left to right). The zero represents the Fermi energy level.
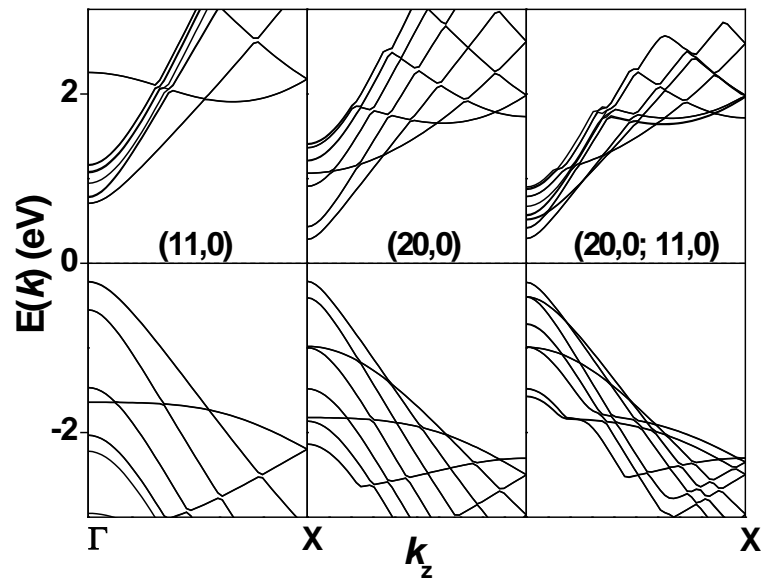

Figure 4.9 Energy band structure of (11,0), (20,0) and (20;11,0) (left to right). The zero represents the Fermi energy level.
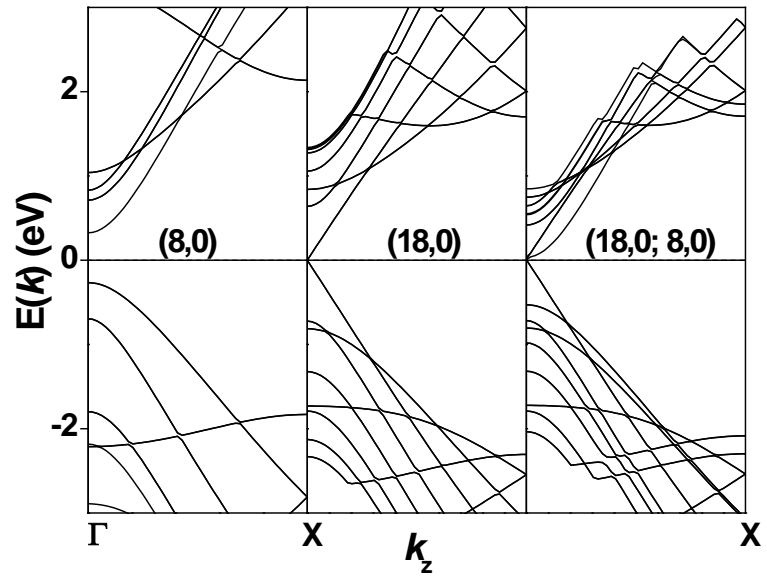
Figure 4.10 Energy band structure of (8,0), (18,0) and (18;8,0) (left to right). The zero represents the Fermi energy level.
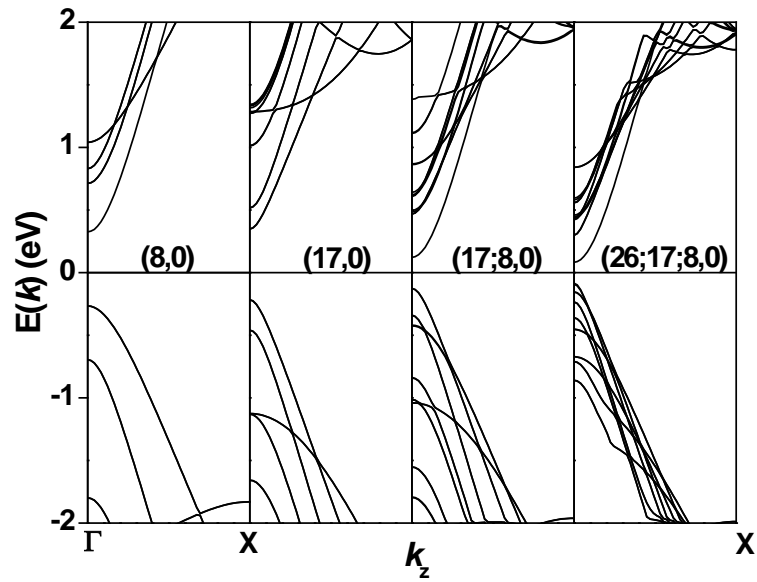

Figure 4.11 Energy band structure of (8,0), (17,0), (17;8,0) and (26;17;8,0) (left to right). The zero represents the Fermi energy level.

Table 4.1 Summary of the CNT band gap calculations

CNT	Cohesive Energy (E_c)	No. of atoms	E_c/atom (eV/atom)	Lattice Parameter (Å)	Band Gap (eV)
7x0	-251.9108	28	-8.99681429	4.26	0.191
8x0	-289.8749	32	-9.05859063	4.26	0.591
10x0	-365.2914	40	-9.132285	4.27	0.7831
11x0	-402.8091	44	-9.15475227	4.26	0.92
16x0	-589.4975	64	-9.21089844	4.27	0.5573
17x0	-626.6993	68	-9.21616618	4.27	0.5637
19x0	-701.109	76	-9.22511842	4.27	0.4791
20x0	-738.279	80	-9.2284875	4.26	0.4941
25x0	-924.0033	100	-9.240033	4.27	0.3817
26x0	-961.14223	104	-9.24175221	4.26	0.3768
MWCNT					
16x7	-840.925809	92	-9.14049792	4.27	0.0602
16x8	-877.684	96	-9.14254167	4.26	0.3942
17x7	-878.47759	96	-9.15080823	4.27	0.0552
17x8	-916.11003	100	-9.1611003	4.26	0.2479
18x8	-953.557807	104	-9.16882507	4.27	0.001
19x10	-1065.8518	116	-9.18837759	4.27	0.4686
19x11	-1101.93459	120	-9.18278825	4.27	0.354
20x10	-1140.38461	120	-9.19320508	4.26	0.4509
20x11	-1140.47256	124	-9.19735935	4.26	0.5165
26x17x8	1876.723061	204	-9.199622848	4.26	0.1668

Based on the results, Figure 4.2-4.11 and Table 4.1, we can conclude that the band gap for a MWCNT is always equal to the lowest or lower than the band gap of any of its constituent SWCNT. In case of (20;11,0) the band gap of the DWCNT is nearly the same as that of the (20,0). In particular, it is to be noted that the band gap for any MWCNT which has any semi-metallic or metallic SWCNT as one of its wall is always metallic.

In the current study, we have considered two cases; first the inner wall to be metallic or low band gap (7,0) and semiconducting outer walls (16,0) and (17,0) respectively. Second, the outer wall to be metallic (18,0) and the a semiconducting inner wall (8,0). From Figure 4.2, 4.3 and 4.10 it can be seen that the band gap closes at the Γ−point indicating that changes have occurred in this region of the BZ. To gain some insight into this behavior, we have investigated into the band decomposed charge density of (16;7,0) DWCNT at the Γ−point. Figure 4.12 shows the results of the wavefunction based charge density. It is known that the curvature effects in (7,0) is responsible for the lower band gap as can be seen from Figure 4.12 indicating significant $\sigma−\pi$ mixing. In case of (16,0) a small degree of $\sigma−\pi$ mixing can be seen, however in (16;7,0) DWCNT this effect is further enhanced leading to closure of band gap. This can be attributed to the perturbation in charge induced from the inner wall. It is also interesting to note that at the Γ−point of the (16;7,0) DWCNT the conduction band is almost entirely contributed from the inner wall (7,0) where as the valence band is contributed from the outer wall (16,0).

57

The reduction n the band gap in with the addition of concentric walls can be explained as a consequence of the following factors. The π orbitals on each of the constituent wall of the MWCNT are along the direction of the normal at the corresponding atomic sites with the exception of very small diameters where π prbital also has a σ contribution that leads to some deviation from a simple π picture. Regardless of the diameter of the CNT there is atleast a lobe of π like orbital that is normal to its circumference at the atomic sites. In case of multiple walls in a CNT these π orbitals interact with each other, this can be understood from the picture of two atomic orbitals of equal energy when brought together which would otherwise be degenerate states lift degeneracy by splitting of the energy levels and this splitting leads to lowering of the energy band gap in these MWCNT. The splitting of the energy levels in case of π orbitals is of the order of 200meV that is consistent with the observation in case of the MWCNT studied for the current research. The interwall interaction can be further confirmed by analyzing the atomic charges on individual carbon atoms that reveals a small charge transfer from inner to the outer wall. In certain cases there is negligible interaction between the walls of the CNT leading to overall energy band gap being the lowest energy band gap of the constituent walls.

Conduction Band
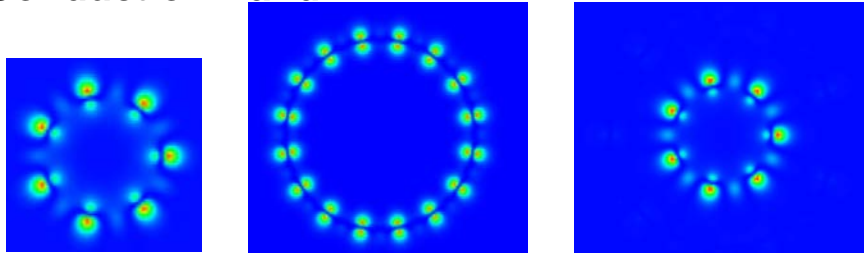
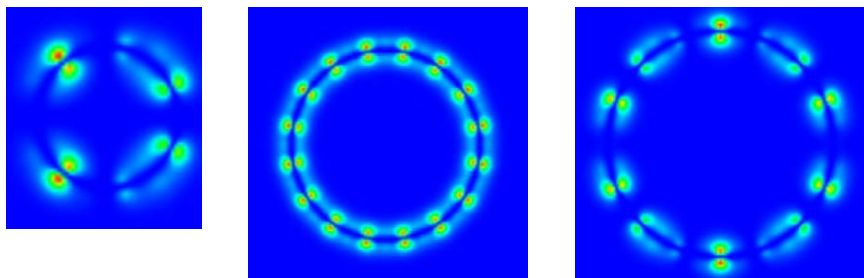**(7x0)**   **(16,0)**   **(16;7,0)**

Valence Band

Figure 4.12 Band decomposed charge density at the Γ−point for (7,0), (16,0) SWCNT

and (16;7,0) DWCNT

In order to understand the behavior of MWCNT we have studied the electronic properties of a three wall zig-zag CNT (26;17;8,0), the inner most wall being (8,0) and the middle wall (17,0) and the outer wall (26,0). The individual band gaps of these SWCNT are listed in Table 4.1. Figure 4.5 and 4.11 show the band structure of the DWCNT (17;8,0) and the MWCNT (26;17;8,0), it is interesting to observe that the band gap of the MWCNT is further reduced from the DWCNT and there by inducing a semi-metallic behavior of the MWCNT. It has been shown in Chapter 3 that there exists an upper limit ~40Å beyond which one will not observe semi-conducting behavior in SWCNT. This observation in conjunction with current finding that the band gap for a MWCNT is always smaller than the band gap of the constituent SWCNT leads us to the conclusion that MWCNT with more than two walls will be either show semi-metallic or metallic behavior. The origin of this metallicity can be described based on the perturbation of charge on the individual walls leading to band gap closure.

Conclusions and Recommendations

One of the central requirements for a device to operate according to predetermined design relies on *apriori* knowledge of the characteristics of the components. Numerous applications for CNTs rely on its novel electrical properties and experimental determination of their chiralities and measurement of their diameters has been a challenge. These characteristics are crucial to its overall performance as they can vary significantly. A third of the single walled CNTs are metallic while the rest are semiconducting. It is extremely difficult to control the chiralities of the CNTs as grown in laboratory. A vital part of the manufacture process is characterization of the synthesized tubes. The experimental measurements fall within the accuracy of the measuring techniques making it extremely difficult to make a unique characterization. However, *apriori* information of their properties can aide in design of reliable and efficient characterization as well as purification processes. Computational solid-state physics provides the tools to probe the properties of these materials with minimal experimental data. Computational studies in conjunction with experiments can help exploit the potential of CNTs.

5.1   SWCNT

Using a first-principles gradient corrected density functional approach, we present a comprehensive study of the geometry and energy band gaps in moderate-gap zig-zag semi-conducting $(n,0)$ carbon nanotubes (CNT) to resolve some of the conflicting findings. Up to (8,0), a strong curvature distortions leads to a strong deviation in energy band gap (ΔE_g) derived from a simple zone folding picture of grapheme based on tight binding calculations. From (10,0) on, the gap dependence on the radius of the tube can be explained surprisingly well with the zone-folding scheme of the graphene bandstructure, if the trigonal shape of the equi-energy lines around the **K**-point is properly taken into account. Our extensive first principle calculations confirm that the $(n,0)$ CNTs fall into two distinct classes depending upon n mod 3 equal to 1 (smaller band gaps) or 2 (larger gaps). The amplitude of the gap oscillations, arising from σ - π mixing, decreases from $n = 10$ to $n = 17$. From $n = 19$ onwards, the gap follows a $\dfrac{1}{d}$ behavior predicted from the simple tight binding π – model with decaying amplitude. The effect of longitudinal strain on the band gap further confirms the existence of two distinct classes: for n mod 3 = 1 or 2, changing ΔE_g by ~100 meV for 1% strain in each case.

5.2   MWCNT

In order to understand the behavior of MWCNT we have studied the electronic properties of a three wall zig-zag CNT. It is interesting to observe that the band gap of the MWCNT is always lower than the its constituent SWCNT band gap there by inducing a metallic behavior of the MWCNT. It has been shown in Chapter 3 that there exists an upper limit ~40Å beyond which one will not observe semi-conducting behavior in SWCNT. This observation in conjunction with current finding that the band gap for a MWCNT is always smaller than the band gap of the constituent SWCNT leads us to the conclusion that MWCNT with multiple walls will be metallic. The origin of this metallicity can be described based on the perturbation of charge on the individual walls leading to band gap closure

5.3   RECOMMENDATIONS

The currents study primarily focused on zig-zag carbon nanotubes and their electronic properties, it has shown unambiguously the existence of two classes of SCNT. However, it has been proposed by other groups that the family behavior is not restricted to the z-g-zag CNTs. This also needs to be rigorously tested from *ab-initio* calculations to put it on firm footing. Also, the mechanism for such behavior in chiral CNTs could be different that the one found in zig-zag SCNT. The changes in these properties lie

within the experimental uncertainty that calls for alternate sources of verification such as Tight Binding models and accurate computational modeling.

References

1. Star, A., et al., *Preparation and Properties of Polymer-Wrapped Single-Walled Carbon Nanotubes.* Angewandte Chemie International Edition in English, 2001. **40**(9): p. 1721-1725.

2. Feynman, R.P., *There's Plenty of Room at the Bottom - An Invitation to Enter a New Field of Physics* in *Engineering & Science,* 1960, California Institute of Technology

3. Kroto, H.W., et al., *C-60 - Buckminsterfullerene.* Nature, 1985. **318**(6042): p. 162-163.

4. Smalley, R.E., *Discovering the Fullerenes*, in *Nobel Lecture*. 1996.

5. Iijima, S., *Helical Microtubules of Graphitic Carbon.* Nature, 1991. **354**(6348): p. 56-58.

6. Michael Ströck, *Types of Carbon Nanotubes*, 2006, Wikimedia Foundation, http://upload.wikimedia.org/wikipedia/commons/5/53/Types_of_Carbon_Nanotubes.png, Accessed on July 10, 2008.

7. Yu, M.-F., et al., *Tensile Loading of Ropes of Single Wall Carbon Nanotubes and their Mechanical Properties.* Physical Review Letters, 2000. **84**(24): p. 5552.

8. Yu, M.-F., et al., *Strength and Breaking Mechanism of Multiwalled Carbon Nanotubes Under Tensile Load.* Science, 2000. **287**(5453): p. 637-640.

9.   Li, F., et al., *Tensile strength of single-walled carbon nanotubes directly measured from their macroscopic ropes.* Applied Physics Letters, 2000. **77**(20): p. 3161-3163.

10.   Frankland, S.J.V., et al., *The Stress-Strain Behavior of Polymer-Nanotube Composites from Molecular Dynamics Simulation.* Composites Science and Technology, 2003. **63**(11): p. 1655-1661.

11.   Frankland, S.J.V., et al., *Modeling and Characterization of Elastic Constants of Functionalized Nanotube Materials*, in *Mechanical Properties of Nanostructured Materials and Nanocomposites*, I. Ovid'ko, et al., Editors. 2004, Material Research Society: Warrendale, PA. p. Q9.10.1-6.

12.   Frankland, S.J.V., G.M. Odegard, and T.S. Gates. *The Effect of Functionalization on Double-Walled Nanotube Materials*. in *International Symposium on Clusters and Nano-Assemblies: Physical and Biological Systems*. 2003. Richmond, VA.

13.   Odegard, G.M., S.J.V. Frankland, and T.S. Gates. *The Effect of Chemical Functionalization on Mechanical Properties of Nanotube/Polymer Composites*. in *44th AIAA/ASME/ASCE/AHS Structures, Structural Dynamics, and Materials Conference*. 2003. Norfolk, VA.

14.   Odegard, G.M., S.J.V. Frankland, and T.S. Gates, *Effect of Nanotube Functionalization on the Elastic Properties of Polyethylene Nanotube Composites.* AIAA Journal, 2005. **43**(8): p. 1828-1835.

15.   Odegard, G.M., et al. *Constitutive Modeling of Crosslinked Nanotube Materials*. in *45th AIAA/ASME/ASCE/AHS/ASC Structures, Structural Dynamics, and Materials Conference*. 2004. Palm Springs, CA.

16.   Baughman, R.H., A.A. Zakhidov, and W.A. de Heer, *Carbon Nanotubes--the Route Toward Applications.* Science, 2002. **297**(5582): p. 787-792.

17.   de Heer, W.A., A. Châtelain, and D. Ugarte, *A Carbon Nanotube Field-Emission Electron Source.* Science, 1995. **270**(5239): p. 1179-1180.

18.   Kong, J., et al., *Nanotube Molecular Wires as Chemical Sensors.* Science, 2000. **287**(5453): p. 622-625.

19.   Balasubramanian, K. and M. Burghard, *Biosensors based on carbon nanotubes.* Analytical and Bioanalytical Chemistry, 2006. **385**(3): p. 452-468.

20.   Madden, J.D., *MATERIALS SCIENCE: Artificial Muscle Begins to Breathe.* Science, 2006. **311**(5767): p. 1559-1560.

21.   Ebron, V.H., et al., *Fuel-Powered Artificial Muscles.* Science, 2006. **311**(5767): p. 1580-1583.

22.   Hohenberg, P. and W. Kohn, *Inhomogeneous Electron Gas.* Physical Review, 1964. **136**.

23.   Hamada, N., S. Sawada, and A. Oshiyama, *New One-Dimensional Conductors - Graphitic Microtubules.* Physical Review Letters, 1992. **68**(10): p. 1579-1581.

24.   Mintmire, J.W., D.H. Robertson, and C.T. White, *Properties of Fullerene Nanotubules.* Journal of Physics and Chemistry of Solids, 1993. **54**(12): p. 1835-1840.

25. White, C.T., D.H. Robertson, and J.W. Mintmire, *Helical and Rotational Symmetries of Nanoscale Graphitic Tubules.* Physical Review B, 1993. **47**(9): p. 5485-5488.

26. Jishi, R.A., et al., *Electronic and Lattice Properties of Carbon Nanotubes.* Journal of the Physical Society of Japan, 1994. **63**(6): p. 2252-2260.

27. Dresselhaus, M.S., G. Dresselhaus, and R. Saito, *Physics of Carbon Nanotubes.* Carbon, 1995. **33**(7): p. 883-891.

28. Saito, R., G. Dresselhaus, and M.S. Dresselhaus, *Physical Properties of Carbon Nanotubes.* 1998: World Scientific Publishing Company

29. Odom, T.W., et al., *Atomic structure and electronic properties of single-walled carbon nanotubes.* Nature, 1998. **391**(6662): p. 62-64.

30. Wildoer, J.W.G., et al., *Electronic structure of atomically resolved carbon nanotubes.* Nature, 1998. **391**(6662): p. 59-62.

31. Zhang, Z. and C.M. Lieber, *Nanotube structure and electronic properties probed by scanning tunneling microscopy.* Applied Physics Letters, 1993. **62**: p. 2792-2794

32. Kim, P., et al., *Electronic Density of States of Atomically Resolved Single-Walled Carbon Nanotubes: Van Hove Singularities and End States.* Physical Review Letters, 1999. **82**: p. 1225-1228

33. Saito, R., G. Dresselhaus, and M.S. Dresselhaus, *Trigonal warping effect of carbon nanotubes.* Physical Review B, 2000. **61**(4): p. 2981-2990.

34. Yorikawa, H. and S. Muramatsu, *Chirality Dependence of Energy Gaps of Semiconducting Nanotubules.* Solid State Communications, 1995. **94**(6): p. 435-437.

35. Reich, S. and C. Thomsen, *Chirality dependence of the density-of-states singularities in carbon nanotubes.* Physical Review B, 2000. **62**(7): p. 4273-4276.

36. Yorikawa, H. and S. Muramatsu, *Energy Gaps of Semiconducting Nanotubules.* Physical Review B, 1995. **52**(4): p. 2723-2727.

37. Bachilo, S.M., et al., *Structure-assigned optical spectra of single-walled carbon nanotubes.* Science, 2002. **298**(5602): p. 2361-2366.

38. Gulseren, O., T. Yildirim, and S. Ciraci, *Systematic ab initio study of curvature effects in carbon nanotubes.* Physical Review B, 2002. **65**(15).

39. D'yachkov, P.N. and H. Hermann, *Electronic structure and interband transitions of semi-conducting carbon nanotubes.* Journal of Applied Physics, 2004. **95**(1).

40. Fantini, C., et al., *Optical transition energies for carbon nanotubes from resonant Raman spectroscopy: Environment and temperature effects.* Physical Review Letters, 2004. **93**(14): p. -.

41. Fantini, C., et al., *One-dimensional character of combination modes in the resonance Raman scattering of carbon nanotubes.* Physical Review Letters, 2004. **93**(8): p. -.

42. Telg, H., et al., *Chirality distribution and transition energies of carbon nanotubes.* Physical Review Letters, 2004. **93**(18): p. -.

43. Telg, H., et al., *Chirality distribution and transition energies of carbon nanotubes.* Physical Review Letters, 2004. **93**(17): p. -.

44. Reich, S., et al., *Tight-binding description of graphene.* Physical Review B, 2002. **66**(3): p. -.

45. Kozinsky, B. and N. Marzari, *Static dielectric properties of carbon nanotubes from first principles.* Physical Review Letters, 2006. **96**(16): p. -.

46. Perdew, J.P., *Density-functional approximation for the correlation energy of the inhomogeneous electron gas.* Physical Review B, 1986. **33**(12): p. 8822.

47. Perdew, J.P. and W. Yue, *Accurate and simple density functional for the electronic exchange energy: Generalized gradient approximation.* Physical Review B, 1986. **33**(12): p. 8800.

48. Department, T.P., *Vienna Ab-initio Simulation Package*.

49. Capaz, R.B., et al., *Temperature dependence of the band gap of semiconducting carbon nanotubes.* Physical Review Letters, 2005. **94**(3): p. -.

50. Machón, M., S. Reich, and C. Thomsen, *Strong electron-phonon coupling of the high-energy modes of carbon nanotubes.* Physical Review B, 2006. **74**: p. 205423-1 - 205423-4.

51. Sfeir, M.Y., et al., *Optical spectroscopy of individual single-walled carbon nanotubes of defined chiral structure.* Science, 2006. **312**(5773): p. 554-556.

52.   Blase, X., et al., *Hybridization Effects and Metallicity in Small Radius Carbon Nanotubes.* Physical Review Letters, 1994. **72**(12): p. 1878-1881.

53.   Okada, S. and A. Oshiyama, *Curvature-induced metallization of double-walled semiconducting zigzag carbon nanotubes.* Physical Review Letters, 2003. **91**(21): p. -.

54.   Li, L.X., et al., *Synthesis and characterization of double-walled carbon nanotubes from multi-walled carbon nanotubes by hydrogen-arc discharge.* Carbon, 2005. **43**(3): p. 623-629.

55.   Ren, W.C., et al., *Morphology, diameter distribution and Raman scattering measurements of double-walled carbon nanotubes synthesized by catalytic decomposition of methane.* Chemical Physics Letters, 2002. **359**(3-4): p. 196-202.

56.   Zhao, Z.G., et al., *The growth of multi-walled carbon nanotubes with different morphologies on carbon fibers.* Carbon, 2005. **43**(3): p. 663-665.

Appendix A

The next 14 pages are the copyright permission for Figure 1.1 distributed under GFDL.

0. PREAMBLE

The purpose of this License is to make a manual, textbook, or other functional and useful document "free" in the sense of freedom: to assure everyone the effective freedom to copy and redistribute it,with or without modifying it, either commercially or noncommercially. Secondarily, this License preserves for the author and publisher a way to get credit for their work, while not being considered responsible for modifications made by others.

This License is a kind of "copyleft", which means that derivative works of the document must themselves be free in the same sense. It complements the GNU General Public License, which is a copyleft license designed for free software. We have designed this License in order to use it for manuals for free software, because free software needs free

documentation: a free program should come with manuals providing the same freedoms that the software does. But this License is not limited to software manuals; it can be used for any textual work, regardless of subject matter or whether it is published as a printed book. We recommend this License principally for works whose purpose is instruction or reference.

1. APPLICABILITY AND DEFINITIONS

This License applies to any manual or other work, in any medium, that contains a notice placed by the copyright holder saying it can be distributed under the terms of this License. Such a notice grants a world-wide, royalty-free license, unlimited in duration, to use that work under the conditions stated herein. The "Document", below, refers to any such manual or work. Any member of the public is a licensee, and is addressed as "you". You accept the license if you copy, modify or distribute the work in a way requiring permission under copyright law.

A "Modified Version" of the Document means any work containing the Document or a portion of it, either copied verbatim, or with modifications and/or translated into another language.

A "Secondary Section" is a named appendix or a front-matter section of the Document that deals exclusively with the relationship of the publishers or authors of the Document to the Document's overall subject (or to related matters) and contains nothing that could

fall directly within that overall subject. (Thus, if the Document is in part a textbook of mathematics, a Secondary Section may not explain any mathematics.) The relationship could be a matter of historical connection with the subject or with related matters, or of legal, commercial, philosophical, ethical or political position regarding them.

The "Invariant Sections" are certain Secondary Sections whose titles are designated, as being those of Invariant Sections, in the notice that says that the Document is released under this License. If a section does not fit the above definition of Secondary then it is not allowed to be designated as Invariant. The Document may contain zero Invariant Sections. If the Document does not identify any Invariant Sections then there are none.

The "Cover Texts" are certain short passages of text that are listed, as Front-Cover Texts or Back-Cover Texts, in the notice that says that the Document is released under this License. A Front-Cover Text may be at most 5 words, and a Back-Cover Text may be at most 25 words.

A "Transparent" copy of the Document means a machine-readable copy, represented in a format whose specification is available to the general public, that is suitable for revising the document straightforwardly with generic text editors or (for images composed of pixels) generic paint programs or (for drawings) some widely available drawing editor, and that is suitable for input to text formatters or for automatic translation to a variety of formats suitable for input to text formatters. A copy made in

an otherwise Transparent file format whose markup, or absence of markup, has been arranged to thwart or discourage subsequent modification by readers is not Transparent. An image format is not Transparent if used for any substantial amount of text. A copy that is not "Transparent" is called "Opaque".

Examples of suitable formats for Transparent copies include plain ASCII without markup, Texinfo input format, LaTeX input format, SGML or XML using a publicly available DTD, and standard-conforming simple HTML, PostScript or PDF designed for human modification. Examples of transparent image formats include PNG, XCF and JPG. Opaque formats include proprietary formats that can be read and edited only by proprietary word processors, SGML or XML for which the DTD and/or processing tools are not generally available, and the machine-generated HTML, PostScript or PDF produced by some word processors for output purposes only.

The "Title Page" means, for a printed book, the title page itself, plus such following pages as are needed to hold, legibly, the material this License requires to appear in the title page. For works in formats which do not have any title page as such, "Title Page" means the text near the most prominent appearance of the work's title, preceding the beginning of the body of the text.

A section "Entitled XYZ" means a named subunit of the Document whose title either is precisely XYZ or contains XYZ in parentheses following text that translates XYZ in

another language. (Here XYZ stands for a specific section name mentioned below, such as "Acknowledgements", "Dedications", "Endorsements", or "History".) To "Preserve the Title" of such a section when you modify the Document means that it remains a section "Entitled XYZ" according to this definition.

The Document may include Warranty Disclaimers next to the notice which states that this License applies to the Document. These Warranty Disclaimers are considered to be included by reference in this License, but only as regards disclaiming warranties: any other implication that these Warranty Disclaimers may have is void and has no effect on the meaning of this License.

2. VERBATIM COPYING

You may copy and distribute the Document in any medium, either commercially or noncommercially, provided that this License, the copyright notices, and the license notice saying this License applies to the Document are reproduced in all copies, and that you add no other conditions whatsoever to those of this License. You may not use technical measures to obstruct or control the reading or further copying of the copies you make or distribute. However, you may accept compensation in exchange for copies. If you distribute a large enough number of copies you must also follow the conditions in section 3.

You may also lend copies, under the same conditions stated above, and you may publicly display copies.

3. COPYING IN QUANTITY

If you publish printed copies (or copies in media that commonly have printed covers) of the Document, numbering more than 100, and the Document's license notice requires Cover Texts, you must enclose the copies in covers that carry, clearly and legibly, all these Cover Texts: Front-Cover Texts on the front cover, and Back-Cover Texts on the back cover. Both covers must also clearly and legibly identify you as the publisher of these copies. The front cover must present the full title with all words of the title equally prominent and visible. You may add other material on the covers in addition. Copying with changes limited to the covers, as long as they preserve the title of the Document and satisfy these conditions, can be treated as verbatim copying in other respects.

If the required texts for either cover are too voluminous to fit legibly, you should put the first ones listed (as many as fit reasonably) on the actual cover, and continue the rest onto adjacent pages.

If you publish or distribute Opaque copies of the Document numbering more than 100, you must either include a machine-readable Transparent copy along with each Opaque copy, or state in or with each Opaque copy a computer-network location from which the

general network-using public has access to download using public-standard network protocols a complete Transparent copy of the Document, free of added material. If you use the latter option, you must take reasonably prudent steps, when you begin distribution of Opaque copies in quantity, to ensure that this Transparent copy will remain thus accessible at the stated location until at least one year after the last time you distribute an Opaque copy (directly or through your agents or retailers) of that edition to the public.

It is requested, but not required, that you contact the authors of the Document well before redistributing any large number of copies, to give them a chance to provide you with an updated version of the Document.

4. MODIFICATIONS

You may copy and distribute a Modified Version of the Document under the conditions of sections 2 and 3 above, provided that you release the Modified Version under precisely this License, with the Modified Version filling the role of the Document, thus licensing distribution and modification of the Modified Version to whoever possesses a copy of it. In addition, you must do these things in the Modified Version:

A. Use in the Title Page (and on the covers, if any) a title distinct from that of the Document, and from those of previous versions (which should, if there were any, be

listed in the History section of the Document). You may use the same title as a previous version if the original publisher of that version gives permission.

B. List on the Title Page, as authors, one or more persons or entities responsible for authorship of the modifications in the Modified Version, together with at least five of the principal authors of the Document (all of its principal authors, if it has fewer than five), unless they release you from this requirement.

C. State on the Title page the name of the publisher of the Modified Version, as the publisher.

D. Preserve all the copyright notices of the Document.

E. Add an appropriate copyright notice for your modifications adjacent to the other copyright notices.

F. Include, immediately after the copyright notices, a license notice giving the public permission to use the Modified Version under the terms of this License, in the form shown in the Addendum below.

G. Preserve in that license notice the full lists of Invariant Sections and required Cover Texts given in the Document's license notice.

H. Include an unaltered copy of this License.

I. Preserve the section Entitled "History", Preserve its Title, and add to it an item stating at least the title, year, new authors, and publisher of the Modified Version as given on the Title Page. If there is no section Entitled "History" in the Document, create one stating the title, year, authors, and publisher of the Document as given on its Title Page, then add an item describing the Modified Version as stated in the previous sentence.

J. Preserve the network location, if any, given in the Document for public access to a Transparent copy of the Document, and likewise the network locations given in the Document for previous versions it was based on. These may be placed in the "History" section. You may omit a network location for a work that was published at least four years before the Document itself, or if the original publisher of the version it refers to gives permission.

K. For any section Entitled "Acknowledgements" or "Dedications", Preserve the Title of the section, and preserve in the section all the substance and tone of each of the contributor acknowledgements and/or dedications given therein.

L. Preserve all the Invariant Sections of the Document, unaltered in their text and in their titles. Section numbers or the equivalent are not considered part of the section titles.

M. Delete any section Entitled "Endorsements". Such a section may not be included in the Modified Version.

N. Do not retitle any existing section to be Entitled "Endorsements" or to conflict in title with any Invariant Section.

O. Preserve any Warranty Disclaimers.

If the Modified Version includes new front-matter sections or appendices that qualify as Secondary Sections and contain no material copied from the Document, you may at your option designate some or all of these sections as invariant. To do this, add their titles to the list of Invariant Sections in the Modified Version's license notice. These titles must be distinct from any other section titles.

You may add a section Entitled "Endorsements", provided it contains nothing but endorsements of your Modified Version by various parties--for example, statements of peer review or that the text has been approved by an organization as the authoritative definition of a standard.

You may add a passage of up to five words as a Front-Cover Text, and a passage of up to 25 words as a Back-Cover Text, to the end of the list of Cover Texts in the Modified Version. Only one passage of Front-Cover Text and one of Back-Cover Text may be added by (or through arrangements made by) any one entity. If the Document already includes a cover text for the same cover, previously added by you or by arrangement made by the same entity you are acting on behalf of, you may not add another; but you may replace the old one, on explicit permission from the previous publisher that added the old one.

The author(s) and publisher(s) of the Document do not by this License give permission to use their names for publicity for or to assert or imply endorsement of any Modified Version.

5. COMBINING DOCUMENTS

You may combine the Document with other documents released under this License, under the terms defined in section 4 above for modified versions, provided that you include in the combination all of the Invariant Sections of all of the original documents, unmodified, and list them all as Invariant Sections of your combined work in its license notice, and that you preserve all their Warranty Disclaimers.

The combined work need only contain one copy of this License, and multiple identical Invariant Sections may be replaced with a single copy. If there are multiple Invariant Sections with the same name but different contents, make the title of each such section unique by adding at the end of it, in parentheses, the name of the original author or publisher of that section if known, or else a unique number. Make the same adjustment to the section titles in the list of Invariant Sections in the license notice of the combined work.

In the combination, you must combine any sections Entitled "History" in the various original documents, forming one section Entitled "History"; likewise combine any sections Entitled "Acknowledgements", and any sections Entitled "Dedications". You must delete all sections Entitled "Endorsements".

6. COLLECTIONS OF DOCUMENTS

You may make a collection consisting of the Document and other documents released under this License, and replace the individual copies of this License in the various documents with a single copy that is included in the collection, provided that you follow the rules of this License for verbatim copying of each of the documents in all other respects.

You may extract a single document from such a collection, and distribute it individually under this License, provided you insert a copy of this License into the extracted document, and follow this License in all other respects regarding verbatim copying of that document.

7. AGGREGATION WITH INDEPENDENT WORKS

A compilation of the Document or its derivatives with other separate and independent documents or works, in or on a volume of a storage or distribution medium, is called an "aggregate" if the copyright resulting from the compilation is not used to limit the legal rights of the compilation's users beyond what the individual works permit. When the Document is included in an aggregate, this License does not apply to the other works in the aggregate which are not themselves derivative works of the Document.

If the Cover Text requirement of section 3 is applicable to these copies of the Document, then if the Document is less than one half of the entire aggregate, the

Document's Cover Texts may be placed on covers that bracket the Document within the aggregate, or the electronic equivalent of covers if the Document is in electronic form. Otherwise they must appear on printed covers that bracket the whole aggregate.

8. TRANSLATION

Translation is considered a kind of modification, so you may distribute translations of the Document under the terms of section 4. Replacing Invariant Sections with translations requires special permission from their copyright holders, but you may include translations of some or all Invariant Sections in addition to the original versions of these Invariant Sections. You may include a translation of this License, and all the license notices in the Document, and any Warranty Disclaimers, provided that you also include the original English version of this License and the original versions of those notices and disclaimers. In case of a disagreement between the translation and the original version of this License or a notice or disclaimer, the original version will prevail.

If a section in the Document is Entitled "Acknowledgements", "Dedications", or "History", the requirement (section 4) to Preserve its Title (section 1) will typically require changing the actual title.

9. TERMINATION

You may not copy, modify, sublicense, or distribute the Document except as expressly provided for under this License. Any other attempt to copy, modify, sublicense or distribute the Document is void, and will automatically terminate your rights under this License. However, parties who have received copies, or rights, from you under this License will not have their licenses terminated so long as such parties remain in full compliance.

10. FUTURE REVISIONS OF THIS LICENSE

The Free Software Foundation may publish new, revised versions of the GNU Free Documentation License from time to time. Such new versions will be similar in spirit to the present version, but may differ in detail to address new problems or concerns. See http://www.gnu.org/copyleft/.

Each version of the License is given a distinguishing version number. If the Document specifies that a particular numbered version of this License "or any later version" applies to it, you have the option of following the terms and conditions either of that specified version or of any later version that has been published (not as a draft) by the Free Software Foundation. If the Document does not specify a version number of this License, you may choose any version ever published (not as a draft) by the Free Software Foundation.

ADDENDUM: How to use this License for your documents

To use this License in a document you have written, include a copy of the License in the document and put the following copyright and license notices just after the title page: Copyright (c) YEAR YOUR NAME. Permission is granted to copy, distribute and/or modify this document under the terms of the GNU Free Documentation License, Version 1.2 or any later version published by the Free Software Foundation; with no Invariant Sections, no Front-Cover Texts, and no Back-Cover Texts. A copy of the license is included in the section entitled "GNU Free Documentation License".

If you have Invariant Sections, Front-Cover Texts and Back-Cover Texts, replace the "with...Texts." line with this: with the Invariant Sections being LIST THEIR TITLES, with the Front-Cover Texts being LIST, and with the Back-Cover Texts being LIST.

If you have Invariant Sections without Cover Texts, or some other combination of the three, merge those two alternatives to suit the situation.

If your document contains nontrivial examples of program code, we recommend releasing these examples in parallel under your choice of free software license, such as the GNU General Public License, to permit their use in free software.